

Oligonucleotide Analogues with Integrated Bases and Backbone

Part 28¹⁾

Hydrazide- and Amide-Linked Analogues. 2. Di-, Tetra-, Octa-, and Decamers: Synthesis and Association

by **Fabio De Giacomo**²⁾, **Manuel Peifer**²⁾, **Zrinka Rajic**³⁾, and **Andrea Vasella**^{*}

Laboratorium für Organische Chemie, ETH Zürich, Wolfgang-Pauli Strasse 10, CH-8093 Zürich
(e-mail: vasella@org.chem.ethz.ch)

The protected hydrazide-linked uracil- and adenine-derived tetranucleoside analogues **17**, **19**, and **21** were synthesized in solution by coupling the dimeric hydrazines **6** and **10** with the carboxylic acids **7**, **11**, and **16**. These hydrazines and acids were obtained by partially deprotecting the hydrazines **5**, **9**, and **15**, and these were prepared by coupling the hydrazines **3** and **14** with the carboxylic acids **4** and **8**. The crystal structure analysis of the fully protected UU dimer **5** showed the formation of an antiparallel cyclic duplex with the uracil units H-bonded *via* H–N(3) and O=C(2). Stacking interactions were observed between the uracil units with a buckle twist of 30.9°, and between the uracil unit II and the fluoren-9-yl group of Fmoc (= 9*H*-fluoren-9-yl)methoxycarbonyl). The hydrazide H–N(3') and the C=O group of Fmoc form an intramolecular H-bond. The uracil- and adenine-derived, water-soluble hydrazide-linked self-complementary octamers **23–32** and the non-self-complementary uracil derived decamer **33** were obtained by coupling the carboxylic acids **4** and **8** on a solid support. ¹H-NMR Analysis in CDCl₃, mixtures of CDCl₃ and (D₆)DMSO, and (D₈)THF showed that the partially deprotected dimers **5**, **6**, **12**, and **13** form weakly associated linear duplexes. The partially deprotected tetramers **17** and **18** do not associate. The hydrazide-linked octamers **23–32** do not stack in aqueous solution, and the non-self-complementary decamer **33** does not stack with the complementary strands of DNA **43** and RNA **42**. The Cbz-protected amide-linked octamers **51–56** derived from uracil, adenine, cytosine, and guanine were obtained as the main products by solid-phase synthesis from the carboxylic acids **46–49**. The fully deprotected amide-linked octamers proved insoluble, and could neither be purified nor analysed.

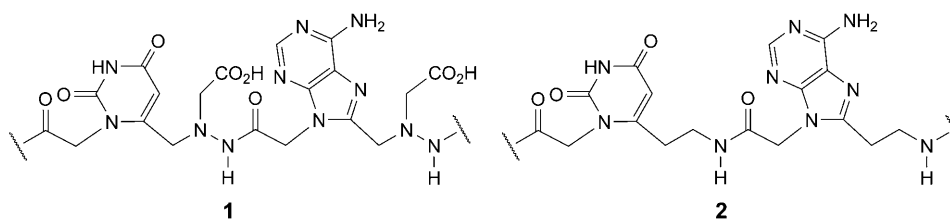
Introduction. – We already detailed the reasons for our interest in novel oligonucleotide analogues with integrated bases and backbone (ONIBs) [2]. Briefly put, we wished to modify the structure of previously synthesized ONIBs [3–12] in omitting the ribosyl moiety and choosing an advantageous linker to simplify the synthesis. We thereby intended to further explore the limits within which the structure of ONIBs can be varied while maintaining their pairing properties, and to obtain ONIBs that pair in aqueous solution. To reach these goals, we designed ONIBs characterized by hydrazide and by amide linkers, as illustrated by the general structures **1** and **2**, respectively.

We planned to prepare di- and tetramers in solution and higher oligomers on a solid support, to combine the advantages of each method [13][14]. Similarly to the synthesis

¹⁾ Part 27 [1].

²⁾ Taken in part from the Ph.D. thesis of *M. P.* and *F. D. G.*

³⁾ Doctoral exchange student, on leave of absence from the University of Zagreb.



of peptide nucleic acids (PNAs), the synthesis of the higher oligomers could follow either a Boc- [15] or an Fmoc-based [16] strategy; we opted for the Fmoc strategy that allows for deprotection under milder conditions.

The synthesis in solution should lead to sufficient amounts of di- and tetramers to analyse their association in organic solvents by $^1\text{H-NMR}$ spectroscopy, as described for earlier types of ONIBs [4][8][9][17]. Much smaller amounts of material are obtained by synthesis on solid support, and the association of the self-complementary octamers in aqueous solution has to be analysed on the basis of their temperature-dependent UV spectra [18] to assess π -stacking, the major stabilising force in aqueous solvents [19]. We also intended to test for cross-pairing of a non-self complementary hydrazide-linked decamer with complementary strands of RNA and DNA.

We already reported the synthesis of the required monomeric building blocks [2], and now describe the synthesis of uracil- and adenine-derived, hydrazide-linked di-, tetra-, octa-, and decamers and of amide-linked octamers.

Results and Discussion. – Synthesis of the Hydrazide-Linked Dimers in Solution.

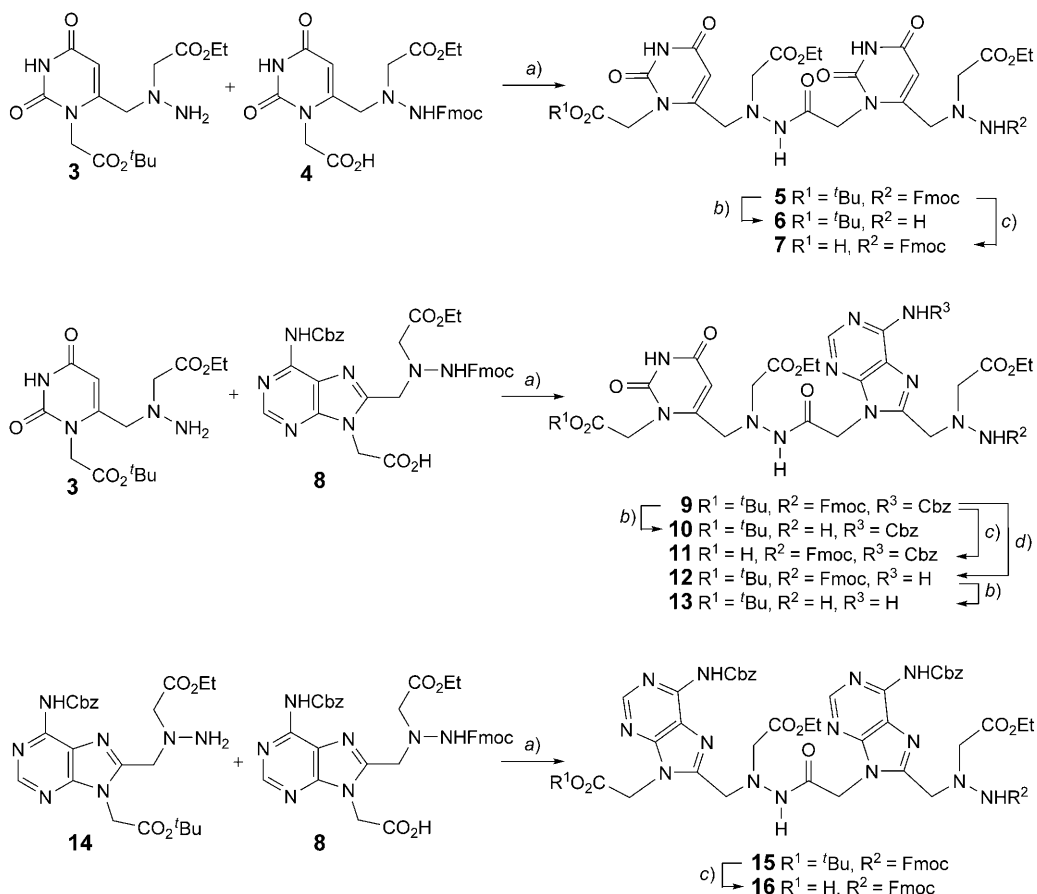
The hydrazide-linked fully protected UU dimer **5**, UA dimer **9**, and AA dimer **15** were synthesized by *N*-acylation of the previously described uracil-derived hydrazine **3** and the adenine-derived analogue **14** with the carboxylic acids **4** and **8** [2] (*Scheme 1*)⁴, using HBTU⁵ as coupling agent in combination with *Hünig*'s base in DMF. The Fmoc groups were removed with piperidine in DMF, and the *tert*-butyl esters were cleaved by the action of trifluoroacetic acid (TFA) in the presence of Et_3SiH in CH_2Cl_2 , adding a large excess of Et_3SiH when cleaving the *tert*-butyl ester group of Cbz-protected dimers to avoid partial loss of the Cbz groups [2][16] that were removed by Pd-catalyzed hydrogenolysis.

Coupling the hydrazine **3** with the benzotriazol-1-yl ester derived from acid **4** (*Scheme 1*) yielded 98% of the fully protected UU dimer **5**. We similarly coupled the hydrazines **3** and **14** with the acid **8** to obtain the fully protected UA dimer **9** (77%) and

⁴) The structures of the hydrazide- and amide-linked oligonucleotide analogues are drawn with the linker connecting C(6) or C(8) of a nucleobase on the left to N(1) or N(9) of the nucleobase on the right, by analogy to the drawing convention adopted for the other ONIBs [3–5][7–12]. The base sequence is, therefore, given from the C- to the N-terminus, in contradistinction to peptides and PNAs [20], with the base units numbered (roman numerals) from left to right.

⁵) *O*-(Benzotriazole-1-yl)-1,1,3,3-tetramethyluronium hexafluorophosphate. There was no advantage in using the more expensive HATU (= *O*-(7-Aza-1*H*-benzotriazole-1-yl)-1,1,3,3-tetramethyluronium hexafluorophosphate).

Scheme 1



a) HBTU, HOBT, $i\text{Pr}_2\text{NEt}$, DMF; 98% of **5**; 77% of **9**. b) Piperidine, DMF; 99% of **6**; 80% of **10**; 80% of **13**. c) F_3CCOOH (TFA), Et_3SiH , CH_2Cl_2 ; 99% of **7**; 98% of **11**; 69% of **16**. d) 1. $\text{Pd}(\text{OAc})_2$, H_2 , $\text{MeOH}/\text{CH}_2\text{Cl}_2$ 1:1; 2. **9**, $\text{MeOH}/\text{CH}_2\text{Cl}_2$ 1:1; 94%.

AA dimer **15**, respectively. Removing the Fmoc group of **5** yielded 99% of the dimeric hydrazine **6**. Similarly, **9** yielded 80% of **10**.

Cleaving the *tert*-butyl esters **5** and **9** afforded the dimeric carboxylic acids **7** (98%) and **11** (84%), respectively. Crude **7** was sufficiently pure for the next step, while acid **11** was purified by MPLC. Cleaving the *tert*-butyl ester **15** gave acid **16** (78% from **14**). Pd-Catalysed debenzoyloxycarbonylation of **9** yielded 94% of **12**. The reaction was slow and required 30 h for completion, even in the presence of a stoichiometric amount of $\text{Pd}(\text{OAc})_2$. Removing the Fmoc group of **12** provided the hydrazine **13** in almost quantitative yield.

Slow evaporation of a solution of **5** in EtOH afforded crystals that were suitable for X-ray analysis (*Fig. 1*)⁶⁾.

Each molecule of **5** in the unit cell is H-bonded *via* H–N(3) and O=C(2) to the enantiomeric conformer ('invertomer', with the tetrahedral N-atom of the hydrazide group as a centre of chirality), forming an antiparallel cyclic duplex (*Fig. 1, a*). The planes of the uracil rings of units I and II form an angle of 30.9°, corresponding to a buckle twist. The O=C(4) group of units I in the duplex accept a H-bond from H₂O, whereas the O=C(4) group of units II accept a H-bond from EtOH.

The fluorenyl and the uracil group of unit II of **5** in adjacent unit cells stack, with a distance of 3.4 Å between the planes of the aromatic rings (*Fig. 1, b*). The hydrazide N(3')–H forms an intramolecular H-bond to the Fmoc C=O group (distance NH...O = 2.1 Å). A further H-bond is suggested by the distance of 2.3 Å between H–C(5) and O=C(4) of units II [21].

A comparison of the conformation of crystalline **5** with the calculated conformation of a hydrazide-linked dimer lacking the fluorenyl group is far from obvious, considering the stacking interactions and the intramolecular H-bond in the crystal. Even so, the torsion angles κ , ι_1 , ι_2 , ε_1 , ε_2 , λ , and ζ of **5** in the solid state agree reasonably well with the calculated torsion angles for the cyclic duplex ($\leq 23^\circ$) [2] (*Table*), with a significant deviation (of 42°) for the torsion angle ξ .

Table. Torsion Angles for the Crystal Structure of **5** and Predicted Torsion Angles for the Hydrazide Linker

Torsion Angle	Observed in the Crystal Structure of 5 [°]	Predicted [2] [°]
κ	+58	+70
ι_1	+52	+60
ι_2	+174	180
ε_1	–140	–120
ε_2	+97	+120
λ	180	180
ξ	–28	–70
ζ	+115	+100

The torsion angles ε_1 , ε_2 , and λ confirm the expected (*Z*)-*syn*-conformation of the hydrazide, and the values found for ι_1 and ι_2 confirm the expected antiperiplanar orientation of C(6/I) and CH₂(1'') [2].

The intermediate synperiplanar/synclinal arrangement of NH(3') and N(1/II) ($\xi = -28^\circ$) may well result from the intramolecular H-bond between N–H(3') and the carbamate C=O group. This H-bond can no longer be formed when the torsion angle ξ in the crystal structure is changed from the observed -28° to the calculated -70° .

⁶⁾ The crystallographic data have been deposited with the *Cambridge Crystallographic Data Centre* as deposition No. CCDC-811879. Copies of the data can be obtained free of charge *via* http://www.ccdc.cam.ac.uk/data_request/cif (or from the *Cambridge Crystallographic Data Centre*, 12 Union Road, Cambridge CB21EZ (fax: +44(1223)336033; e-mail: deposit@ccdc.cam.ac.uk).

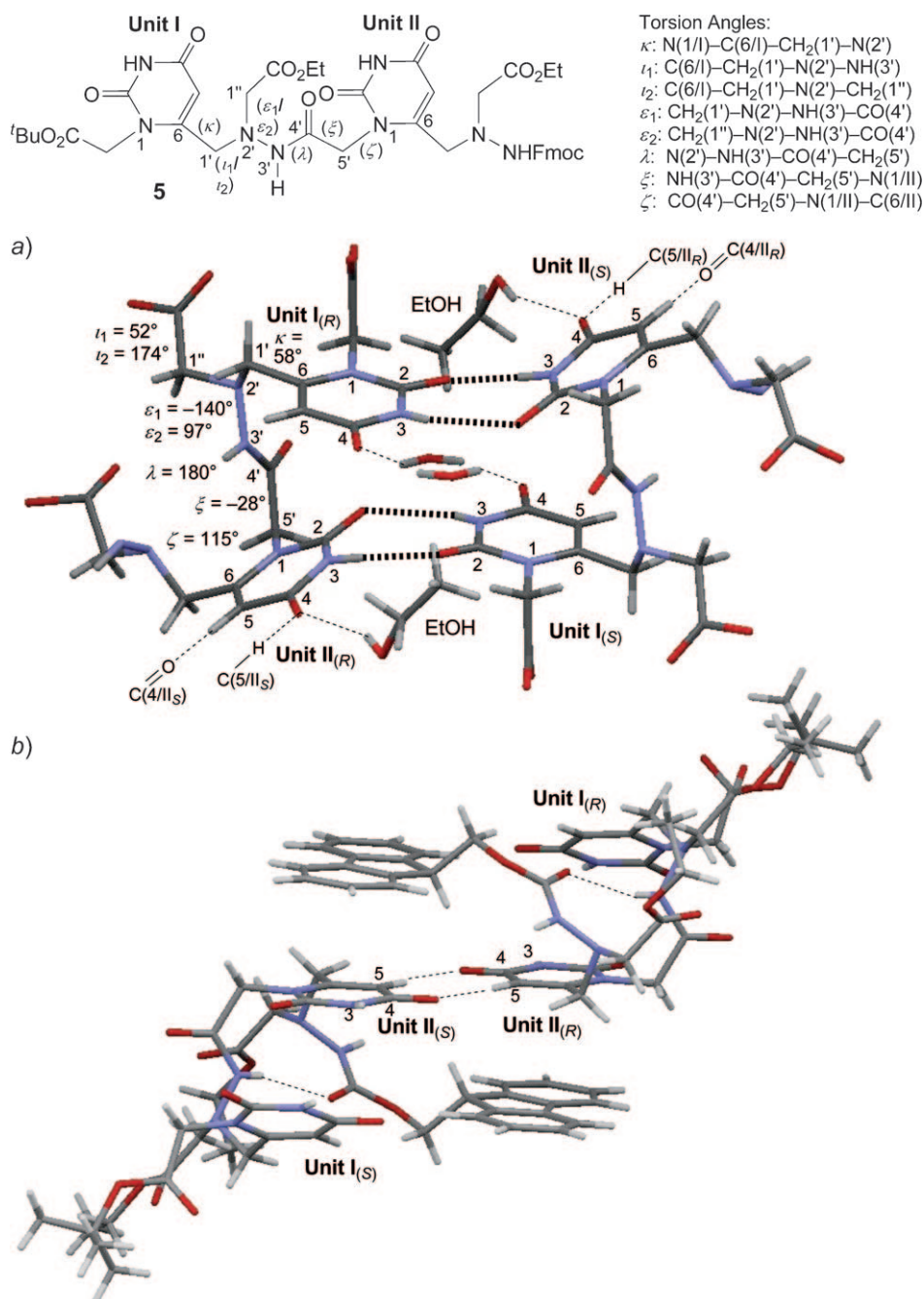


Fig. 1. a) Pairing between the enantiomers (invertomers) of **5** in a cyclic duplex involving H–N(3) and O=C(2) of units I and II (bold dashed lines); H-bonds between enantiomers of **5** involving H–C(5) and O=C(4) of units II (dashed lines); H-bonds of O=C(4/I) with H₂O, and O=C(4/II) with EtOH (dashed lines); values for the torsion angles of the hydrazide linker. The 'Bu, Et, and Fmoc groups are omitted for clarity. b) Stacking of the fluorenyl groups and uracil units II of enantiomers of **5**; intermolecular H-bonds between H–C(5) and O=C(4) of units II of the enantiomers of **5**; intramolecular H-bonds between H–N(3') and the carbamate C=O group.

To check for stacking interactions in solution, we recorded UV spectra of **5** in EtOH and CHCl₃ while varying the temperature. Specific stacking interactions in CHCl₃ were expected to go along with a strong association *via* H-bonding. As the association proved weak (see below), suggesting the formation of mostly linear duplexes, stacking interactions were not considered specific. The data are discussed below, in the context of the analyses of the self-association of **5** in solution.

Solution Synthesis of Hydrazone-Linked Tetramers. The hydrazone-linked UUUU tetramers **17** and **18**, the UAUA tetramers **19** and **20**, and the UUAU tetramers **21** and **22** were synthesized similarly as the dimers (*Scheme 2*). We coupled the dimeric hydrazines **6** and **10** with the dimeric carboxylic acids **7**, **11**, and **16** to provide the fully protected U₄ tetramer **17** (69%), (UA)₂ tetramer **19** (89%), and U₂A₂ tetramer **21** (72%), respectively. Tetramer **17** proved significantly more polar than dimer **5** and more difficult to purify by silica-gel chromatography. Removing the Fmoc group of **17** provided hydrazone **18**. Isothermal diffusion of Et₂O into a saturated solution of **18** in MeOH precipitated 64% of pure **18**. Hydrogenolysis of **19** and **21** in the presence of a large amount of Pd(OAc)₂ provided 65% of **20** after seven days, and 69% of **22** after six days, respectively, both tetramers requiring purification by MPLC.

Solid-Phase Synthesis of Hydrazone-Linked Octa- and Decamers. 1. *Optimisation of the Reaction Conditions.* We synthesised the hydrazone-linked uracil- and adenine-derived octa- and decamers on the standard *Rink* amide 4-methylbenzhydrylamine (MBHA) polystyrene resin [22]. To establish appropriate reaction conditions, we coupled the uracil-derived monomers **3** and **4** in DMF, NMP (= *N*-methylpyrrolidin-2-one), or DMSO, activating **4** with either HBTU [23], HATU [24], HCTU⁷) [25], or PyBOP⁸) [26], always in combination with *Hünig*'s base. Performing the coupling in DMSO and activating the carboxylic acid with HATU resulted in the cleanest and fastest reaction. The superior properties of DMSO were confirmed by test syntheses on the solid phase using either DMF, NMP/DMSO 8:2 [27], 0.8M LiCl in DMF [28], and DMSO [29]. The *N*-Fmoc groups were removed using DBU⁹). The *N*-termini of the final oligomers were capped by *N*-acetylation with Ac₂O/*Hünig*'s base before their cleavage from the resin with TFA/*Pr*₃SiH 97:3.

2. *Synthesis of Octamers Derived from Uracil and Adenine.* According to our modelling [2], the strength of association of the hydrazone-linked octamers derived from uracil and adenine will depend on the sequence, as the extent of base stacking decreases in the order UA > UU > AA > AU. To test this modelling result, we synthesised the self-complementary (UA)₄ octamer **24**, U₄A₄ octamer **26**, (U₂A₂)₂ octamer **28**, and (A₂U₂)₂ octamer **30**. To evaluate pairing with RNA and DNA, we also synthesised the non-self-complementary U₁₀ decamer **33**.

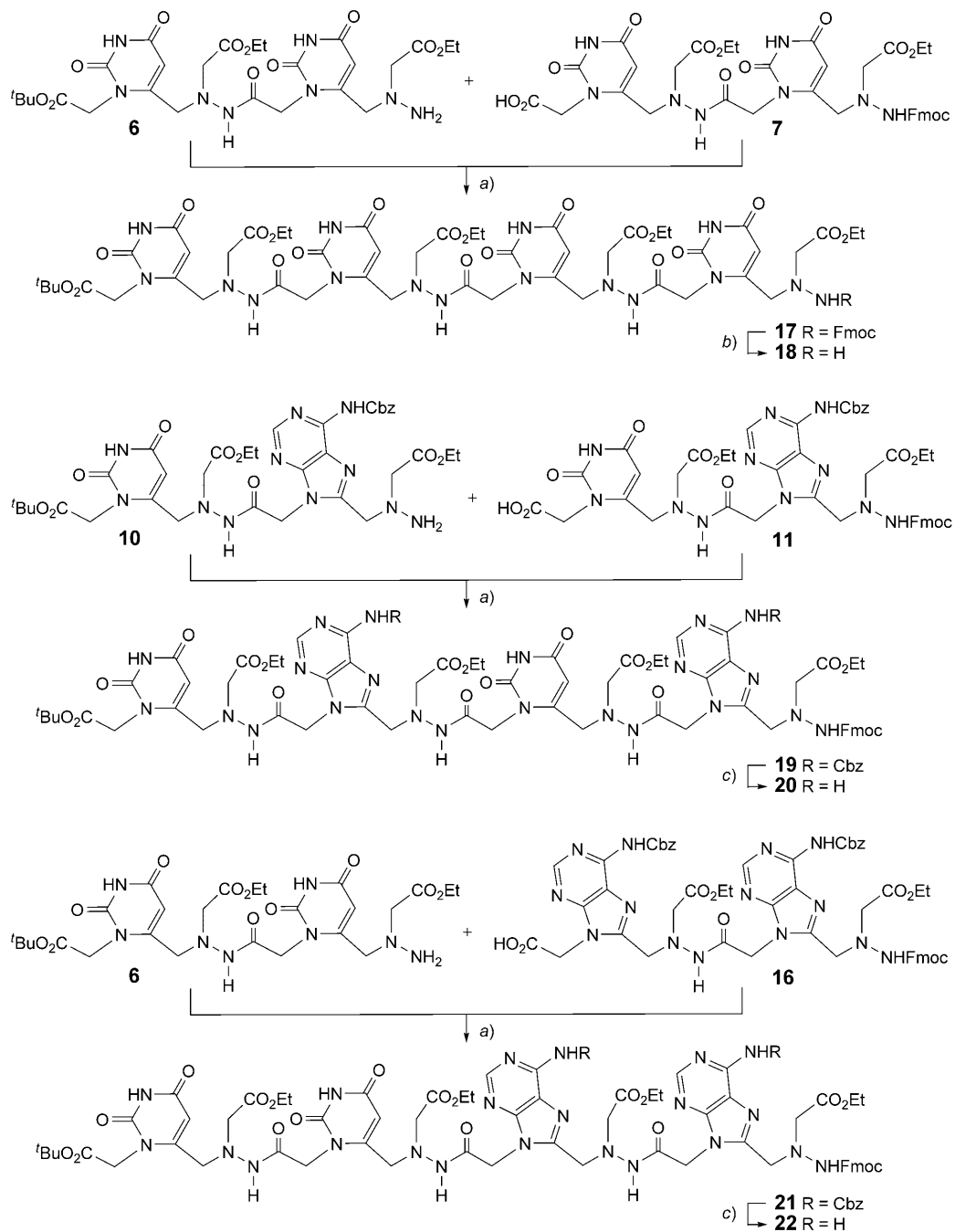
We synthesised the octamers **24**–**30** on the *Rink* amide MBHA resin [22], coupling the acids **4** and **8** with HATU and *Hünig*'s base in DMSO (*Scheme 3*) and removing the Fmoc groups by repetitive short treatments with dilute solutions of DBU, each one followed by washing the resin with DMSO to prevent any addition of the terminal hydrazone to dibenzofulvene (DBF). A high concentration (0.5M) of the activated

⁷) *O*-(6-Chlorobenzotriazol-1-yl)-1,1,3,3-tetramethyluronium hexafluorophosphate.

⁸) (Benzotriazol-1-yloxy)tripyrrolidinophosphonium hexafluorophosphate.

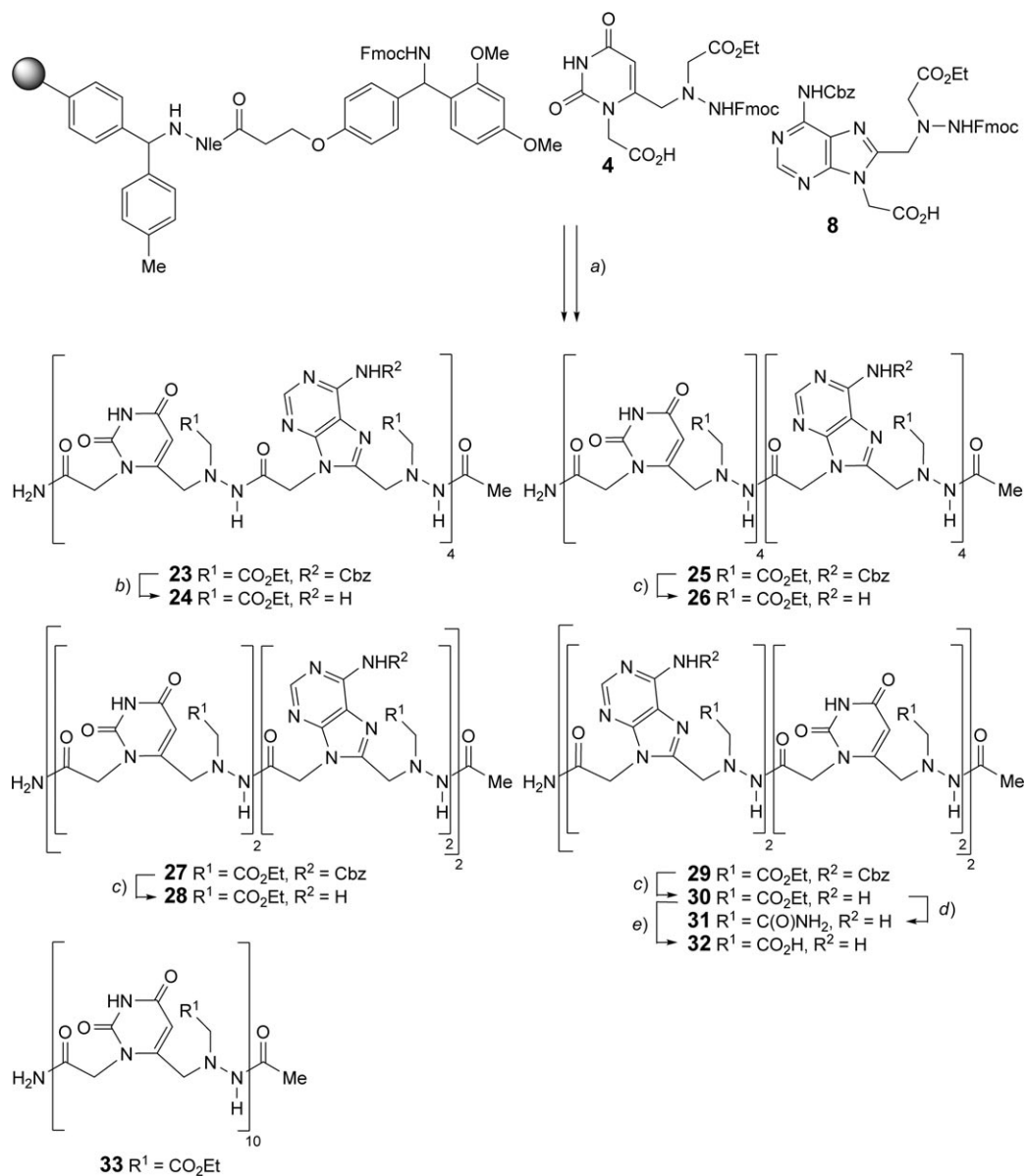
⁹) 1,8-Diazabicyclo[5.4.0]undec-7-ene.

Scheme 2



a) HBTU, HOBT, EtⁿPr₂, DMF; 69% of **17**; 89% of **19**; 72% of **21**. b) Piperidine, DMF; 64%. c) 1. Pd(OAc)₂, H₂, MeOH/CH₂Cl₂ 1:1; 2. **19** or **21**, MeOH/CH₂Cl₂ 1:1; 65% of **20**; 69% of **22**.

Scheme 3



a) Solid-Phase Synthesis. Loading and coupling: *Rink* amide MBHA polystyrene resin, **4** or **8**, HATU, *Hünig's* base, DMSO. *N*-Fmoc deprotection: DBU, DMSO. Capping: Ac_2O , *Hünig's* base, *N*-methylpyrrolidin-2-one (NMP). Cleavage from the resin: $\text{TFA}/\text{Pr}_3\text{SiH}$ 97:3. 2% overall yield of **33**.
b) 1. $\text{Pd}(\text{OAc})_2$, MeOH, H_2 . 2. **23**, MeOH; 5% overall yield of **24**.
c) 1. $\text{TFA}/\text{Pr}_3\text{SiH}$ 97:3, 80° ; 2. *Amberlite IRA-68*, MeCN/ H_2O 1:1; 5% overall yield of **26** and **30**; 8% overall yield of **28**. Yields refer to the loading of the resin (0.72 mmol/g).
d) NH_3 , H_2O ; quant. yield.
e) 1. LiOH, H_2O ; 2. *Amberlite IRA-120*; quant. yield.

carboxylic acid was crucial to drive the couplings to completion. Coupling of the uracil-derived carboxylic acid **4** proceeded cleanly and completely within 4 h. In contrast, coupling of the adenine-derived carboxylic acid **8** was slow, and we detected significant amounts of truncated sequences. The coupling efficiency was neither improved by changing the loading of the resin (as evidenced by similar results obtained from loadings at 0.72 and 0.1 mmol/g of free amino groups on the resin), nor by coupling at 35° rather than at room temperature. When the final capping by acetylation of the N-terminus was omitted, and the polymer-bound oligomer directly exposed to the cleavage conditions (TFA/*i*Pr₃SiH (TIPS) 97:3), we obtained a complex mixture of shorter and longer oligomers, as judged by LC/MS analysis. The mass corresponding to the individual peaks in the chromatogram agreed well with the formation of *trans*-hydrazidation products resulting from the consecutive hydrazinolysis of (protonated) hydrazide groups by the uncapped terminal hydrazino group resulting in the observed mixture of products¹⁰).

Not unexpectedly, the Cbz groups were partially removed during the acidic cleavage of the octamers from the support. The crude octamers **23**, **25**, **27**, and **29** were, therefore, deprotected either by Pd-catalysed hydrogenolysis, or by treatment with TFA/TIPS 97:3 at reflux temperature (*Scheme 3*).

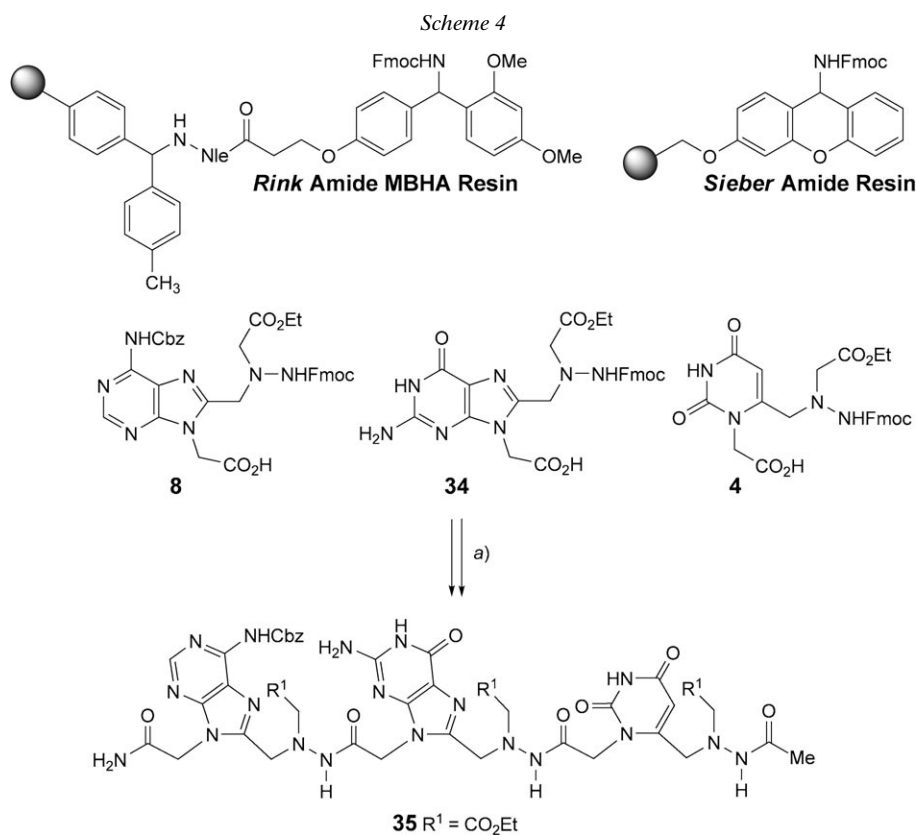
The crude octamers were purified by preparative HPLC. For **24**, **26**, **28**, and **30**, we used an amino phase and for **33** a reversed phase. The low yields of 5–8% for **24–30** may in part be due to incomplete couplings of the adenine-derived monomer **8**, while incomplete detachment from the support is evidenced by the low mass balance of 40–50%. The even lower yield (2%) of **33** results from its difficult chromatographic purification, **33** running close to the truncated sequences.

The self-complementary octameric analogues **24**, **26**, **28**, and **30**, and the non-self-complementary decameric **33** were sufficiently well water-soluble to prepare 10 mM solutions, required to test for stacking in aqueous solution by temperature-dependent UV spectroscopy [18]. To test the influence of the side-chain polarity on the association, we transformed the EtOCO groups of **30** to NH₂CO and to COOH groups (*Scheme 3*). Aminolysis of **30** to **31**, and hydrolysis of **30** to **32** proceeded cleanly, and the products did not require purifying.

3. Attempted Synthesis of Octamers Derived from Cytosine and Guanine. We also applied the optimised conditions for coupling, deprotection, and capping (see above) to synthesize the cytosine- and guanine-derived octamers. Besides the *Rink* amide MBHA resin, we tested the syntheses on a *Sieber* amide polystyrene resin [30] that allows for cleavage of the oligomers under milder conditions, using CH₂Cl₂/TFA 99:1.

Prior to the synthesis of the (C^{Cbz}G)₄ octamer **40**, we tested whether the H₂N–C(2) group of guanine was likely to cause an aminolysis of the hydrazide groups during the cleavage of **40** from the solid support. For this purpose, we synthesized the A^{Cbz}GU trimer **35** (*Scheme 4*), sequentially coupling the hydrazino acids **4**, **8**, and **34** by activation with HATU in the presence of *Hünig*'s base in DMSO, followed by removing the Fmoc groups with dilute solutions of DBU in DMSO, similarly as described for the

¹⁰) An analogous *trans*-amidation, however, was never observed during the synthesis of the amide-linked analogues (see below). This difference is rationalized by the higher electrophilicity of the monoprotonated hydrazides and the nucleophilic properties of the monoprotonated hydrazines.



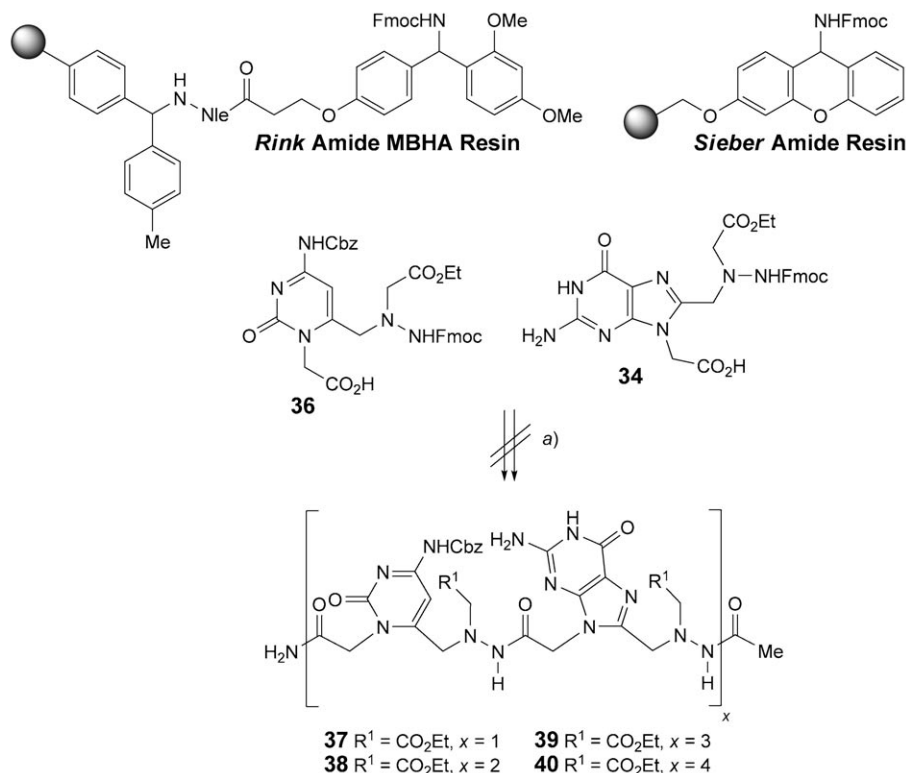
a) Solid-Phase Synthesis. Loading and coupling: *Rink* amide 4-methylbenzhydrylamine (MBHA) polystyrene or the *Sieber* amide polystyrene resin, **8**, **34**, or **4**, HATU, *Hünig's* Base, DMSO. *N*-Fmoc deprotection: DBU, DMSO. Capping: Ac_2O , *Hünig's* base, NMP. Cleavage from the resin: *Rink* amide: TFA/ Pr_3SiH 97:3; *Sieber* amide: $\text{CH}_2\text{Cl}_2/\text{TFA}$ 99:1.

synthesis of the octamers derived from uracil and adenine (see above). The synthesis on a *Rink* amide MBHA resin led to small amounts of shorter and longer oligomers besides the desired **35**, even when the N-terminal hydrazino group was capped, while the synthesis on the *Sieber* amide resin gave exclusively the desired **35**. This observation can be explained by an aminolysis/trans-hydrazidation sequence, analogous to the strand-breaking mechanism described above, but involving the $\text{H}_2\text{N}-\text{C}(2)$ group of guanine.

These side-products were not formed under the mild conditions required for the cleavage of the trimer from the *Sieber* amide resin ($\text{CH}_2\text{Cl}_2/\text{TFA}$ 99:1). We did not observe the acetylation of $\text{C}(2)-\text{NH}_2$ during capping, as it was reported for the synthesis of PNA under similar conditions [31].

We then set off to synthesize the $(\text{C}^{\text{Cbz}}\text{G})_4$ octamer **40** on the *Rink* amide MBHA [22] and also on the *Sieber* amide resin [30] (*Scheme 5*), coupling the acids **36** and **34**, similarly as described for the synthesis of the octamers derived from uracil and adenine.

Scheme 5



a) *Solid-Phase Synthesis*. Loading and coupling: *Rink* amide MBHA polystyrene or the *Sieber* amide polystyrene resin, **36** or **34**, HATU, *Hünig's* base, DMSO. *N*-Fmoc deprotection: DBU, DMSO. Capping: Ac_2O , *Hünig's* base, NMP. Cleavage from the resin: *Rink* amide: TFA/ Pr_3SiH 97:3; *Sieber* amide: $\text{CH}_2\text{Cl}_2/\text{TFA}$ 99:1.

The expected octamer **40** was removed from the *Rink* amide MBHA resin by treatment with TFA/TIPS 97:3, but LC/MS analysis revealed not even a trace of the expected product. The analogous synthesis on the *Sieber* amide resin, monitoring the progress of coupling and deprotection, and the purity of the oligomers resulting after every second cycle by LC/MS analysis, led to the dimer **37** and the tetramer **38**, besides only small amounts of impurities. The hexamer **39**, however, could hardly be identified by LC/MS analysis, and the octamer **40** could not be detected, even after washing the resin with H_2O , MeOH, EtOH, and DMSO. As the LC/MS analysis requires a sufficient solubility of the octamers in MeCN/ H_2O , while their cleavage from the support requires that they are soluble in $\text{CH}_2\text{Cl}_2/\text{TFA}$ 99:1, octamer **40** may well have been formed, but was either not cleaved from the support, or did not dissolve in at least one of the solvent mixtures.

Self-Association of the Hydrazide-Linked UU Dimers. The UU dimer **5** was sufficiently soluble in CDCl_3 to follow the dependence of the chemical shift of the

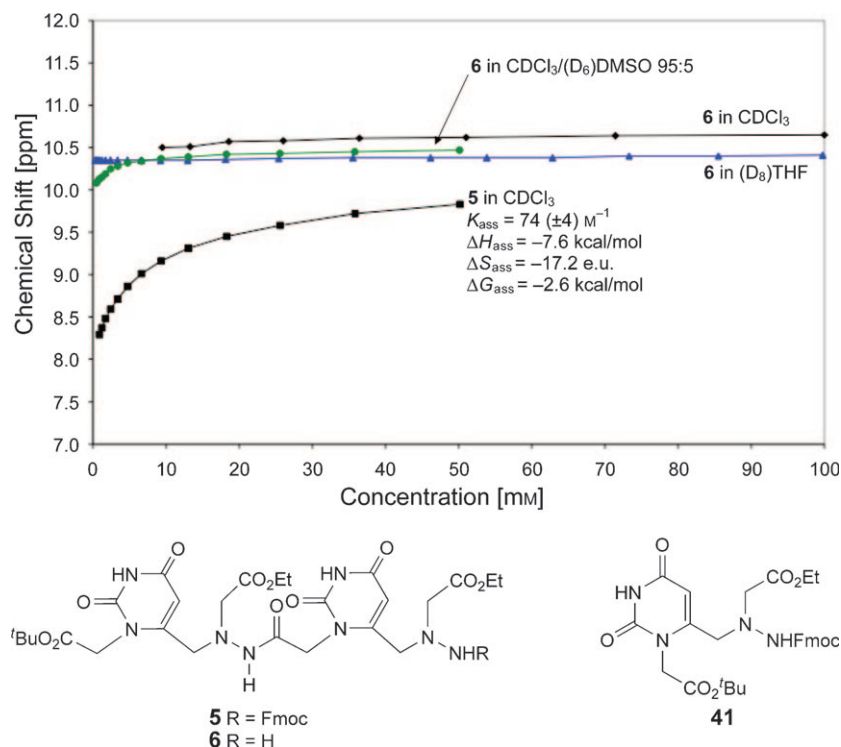


Fig. 2. SCCs for H–N(3) of the UU dimers **5** and **6** in CDCl_3 , $\text{CDCl}_3/(\text{D}_6)\text{DMSO}$ 95:5, and in $(\text{D}_8)\text{THF}$ (solid lines: fitted curve); values for the association constant and thermodynamic parameters of **5** in CDCl_3 ; structure of the U monomer **41**

H–N(3) signals of solutions between the concentrations of 50 and 0.5 mM (Fig. 2). The $^1\text{H-NMR}$ signals of **5** in CDCl_3 were broad, and HMBC spectra did not allow assigning the two H–N(3) signals to the individual uracil units. Their concentration and temperature dependence was, however, very similar, resulting in almost identical association constants and thermodynamic parameters of association, so that only the data derived from one of the H–N(3) are shown in Fig. 2. The association of **5** is weak, with $K_{\text{ass}} = 74(\pm 4) \text{ M}^{-1}$ ¹¹⁾ ($\Delta G_{295} = -2.5 \text{ kcal/mol}$). The enthalpy of association ($\Delta H_{\text{ass}} = -7.6 \text{ kcal/mol}$)¹²⁾ and the shape of the ‘shift-concentration curve’ (SCC) evidence the formation of (one or several) linear duplexes and higher associates. According to the vapour-pressure osmometric (VPO) determination of the apparent molecular mass of **5** at five concentrations between 10 and 50 mM in CHCl_3 , the ratio between the apparent molecular mass and the formula weight increased from 1.23 (10 mM) to 1.74 (50 mM), confirming the (partial) formation of linear duplexes and

¹¹⁾ Determined from the monoplex shift by extrapolation to $c=0$ and from the duplex shift by extrapolation to $c=\infty$.

¹²⁾ Determined by *van't Hoff* analysis, based upon the temperature dependence of the association at a concentration of 10 mM (7–50°).

higher associates. These results do not reflect the H-bonding pattern found in the crystal structure of **5**, where two base pairs of **5** are H-bonded in a cyclic duplex involving the H–N(3) and the O=C(2) groups of the two uracil units.

A ROESY spectrum of **5** was recorded at a 100 mM concentration in CDCl₃ to obtain information about the structure of the associates of **5** in CDCl₃. However, no cross-peaks were detected for the hydrazide NH, H–N(3), H–C(5), or CH₂–N(1), possibly on account of the broad signals. Only weak and insignificant cross-peaks were detected for the (CH₂)₂–N groups and the aromatic H-atoms of the fluorenyl group.

The chemical shift of the hydrazide NH of **5** changed only from 8.66 to 8.16 ppm by lowering the concentration from 50 to 0.5 mM in CDCl₃. These values are typical for 1-acyl-2-alkylhydrazines [32], and evidence that the hydrazide NH is neither involved in a significant intermolecular nor in an intramolecular H-bond, as in the crystal structure of **5**.

We interpret the broad signals in the ¹H-NMR spectra of **5** in CDCl₃ as reflecting rotational equilibria about the hydrazide and the carbamate C–N bonds, and the presence of several weak associates. The assumption of rotational equilibria is confirmed by the ¹H-NMR spectra in (D₆)DMSO, where there should be no association. Although the spectra show sharper peaks, they display two sets of signals, probably due to hydrazide (*E*)- and (*Z*)-isomers, as evidenced by the splitting of the hydrazide NH signal into two peaks in a 6:4 ratio. A similar ratio was found for the other split signals. As the (*Z*) conformation of hydrazides is favoured in polar solvents and with increasing size of the substituents [33], we assume that the (*Z*)-isomers also dominate in (D₆)DMSO. Heating a solution of **5** in (D₆)DMSO to 100° led to coalescence.

The ¹H-NMR spectra of the partially deprotected UU dimer **6** in CDCl₃ showed strong signal broadening. The two H–N(3) resonate as one broad signal that could only be followed in the concentration range of 9.5 to 100 mM. At lower concentrations, it could no longer be detected. The chemical shift of H–N(3) of **6** hardly changed in the mentioned concentration range (Fig. 2). This evidences either a very strong or no association. The downfield shift ($\Delta\delta = 2.7$ ppm) for H–N(3) of **6** relative to the monomer **41** at a concentration of 0.5 mM (Fig. 2) suggests a very strong association of **6**. ¹H-NMR Spectra of **6** were, therefore, recorded in CDCl₃/(D₆)DMSO 95:5, DMSO weakening the association. As expected, sharper signals were observed in this solvent mixture, and the two H–N(3) gave rise to a single broad signal. The H–N(3) signal was followed between 50 and 0.9 mM **6** (Fig. 2), but its chemical shift changed only from 10.47 to 10.16 ppm, and is similar to that of **41** at 0.5 mM in CDCl₃/(D₆)DMSO 95:5 (9.94 ppm), evidencing that **6** hardly associates in this solvent mixture. Considering this result and the observation of a single signal for the two H–N(3), it appears highly improbable that **6** associates strongly in pure CDCl₃. The large value for δ (H–N(3)) in CDCl₃ (10.6 ppm) and its concentration independence within the mentioned concentration range suggest that H–N(3) is involved in an intramolecular H-bond, although the H-bond acceptor is not clear.

The concentration dependence of δ (H–N(3)) of **6** in (D₈)THF (Fig. 2) is characterized by an almost constant chemical shift (10.4 ppm), and the comparison with δ (H–N(3)) of **41** at a concentration of 0.5 mM (10.28 ppm) evidences that **6** does not associate in THF solution.

The $^1\text{H-NMR}$ spectra of **6** in pure (D_6)DMSO exhibited two sets of signals, similarly as observed for **5**, suggesting (*E*)- and (*Z*)-hydrazide isomers. Heating to 100° led to coalescence.

To further test if stacking interactions are present in solutions of either **5** and/or **6**, as compared to those found in the crystal structure of **5**, we recorded the UV spectra of these dimers in EtOH at 0 and 70° , and in CHCl_3 at 0 and 55° (Fig. 3). Stacking interactions were expected to be favoured over H-bonding in EtOH, whereas weaker stacking was expected in CHCl_3 . The UV absorption of both **5** and **6** in both solvents depends on the temperature. The difference of the extinction coefficient of **5** in EtOH at 0 and 70° (Fig. 3, a) at λ_{max} 300 nm ($\Delta\epsilon = 1340 \text{ l} \cdot \text{mol}^{-1} \cdot \text{cm}^{-1}$) indicates inter- or intramolecular stacking involving the fluorenyl group, and $\Delta\epsilon = 3580 \text{ l} \cdot \text{mol}^{-1} \cdot \text{cm}^{-1}$ at λ_{max} 266 nm indicates inter- or intramolecular stacking, either involving the fluorenyl and the uracil groups, or the uracil groups only. A similar temperature dependence of the extinction coefficient of **5** was observed in CHCl_3 solution (Fig. 3, b) at λ_{max} 266 nm ($\Delta\epsilon = 2700 \text{ l} \cdot \text{mol}^{-1} \cdot \text{cm}^{-1}$), but a smaller dependence was found at λ_{max} 300 nm ($\Delta\epsilon = 700 \text{ l} \cdot \text{mol}^{-1} \cdot \text{cm}^{-1}$), suggesting weaker stacking interactions of the fluorenyl group as compared to stacking involving the uracil units. The UV spectra of **6** in EtOH showed also a temperature dependence of the absorption at λ_{max} 266 nm ($\Delta\epsilon = 2060 \text{ l} \cdot \text{mol}^{-1} \cdot \text{cm}^{-1}$) that suggests intra- or intermolecular stacking of the uracil groups. A somewhat smaller temperature dependence was found for the absorption of **6** in CHCl_3 at λ_{max} 266 nm ($\Delta\epsilon = 950 \text{ l} \cdot \text{mol}^{-1} \cdot \text{cm}^{-1}$).

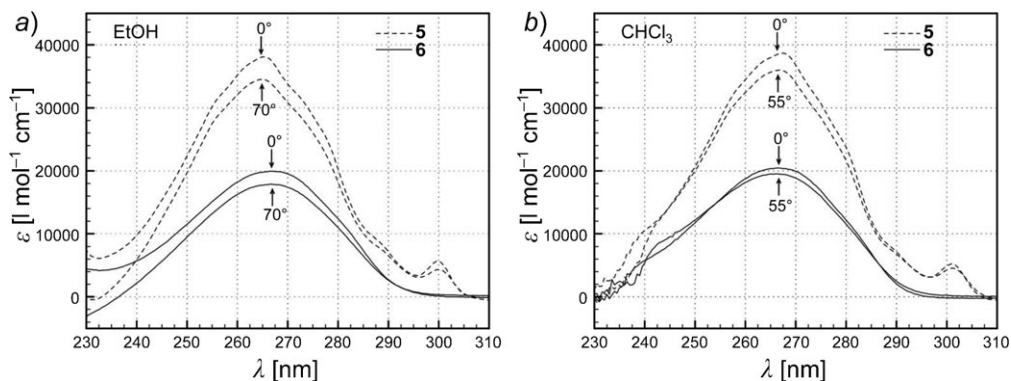


Fig. 3. Extinction coefficient of the UU dimers **5** and **6** in a) 10^{-5} M EtOH solution at 0 and 70° , and in b) 10^{-5} M CHCl_3 solution at 0 and 55°

We conclude that the temperature dependence of the extinction coefficients of **5** and **6** denotes non-specific stacking interactions, as there is no evidence for specific stacking in these cyclic duplexes in view of the evidence for the formation of only linear duplexes and possibly higher associates obtained from the $^1\text{H-NMR}$ analyses discussed above. The similar temperature dependence of the extinction coefficients in EtOH and in CHCl_3 also suggests non-specific stacking interactions.

Self-Association of Hydrazide-Linked UA Dimers. A solution of the UA dimer **12** in CDCl_3 displayed very broad $^1\text{H-NMR}$ signals. The H–N(3) signal of **12** at a

concentration of 50 mM was only just discernible from the base line, resonating between *ca.* 12.4 and *ca.* 11.6 ppm. The shift to *ca.* 12 ppm for H–N(3) of **12** (50 mM), as compared to $\delta(\text{H–N}(3))$ 7.91 ppm of the U monomer **41** (0.5 mM), suggests the involvement of H–N(3) in a H-bond and, therefore, association. However, dilution resulted in the disappearance of the peak, and it was not possible to follow its concentration dependence.

As expected, sharper signals characterize the $^1\text{H-NMR}$ spectra of **12** in $\text{CDCl}_3/(\text{D}_6)\text{DMSO}$ 95:5, and the concentration dependence of $\delta(\text{H–N}(3))$ was determined between 50 and 1.7 mM (Fig. 4). A small association constant $K_{\text{ass}} = 191(\pm 83) \text{ M}^{-1}$ ($\Delta G_{295} = -3.1 \text{ kcal/mol}$) resulted from the shift-concentration data, suggesting the formation of mainly linear aggregates, in agreement with the shape of the SCC and the thermodynamic parameters of association ($\Delta H_{\text{ass}} = -10.1 \text{ kcal/mol}$, $\Delta S_{\text{ass}} = -24.2 \text{ e.u.}$, $\Delta G_{\text{ass}} = -3.0 \text{ kcal/mol}$), as determined by a *van't Hoff* analysis of a 10 mM solution ($T = 7-50^\circ$).

This result leads to the conclusion that the UA dimer **12** associates in CDCl_3 . The shift to lower fields of the H–N(3) signal of **12** in CDCl_3 at a concentration of 50 mM (*ca.* 12.0 ppm) relative to the corresponding *N*-Fmoc-protected UU dimer **5** at the same concentration (9.8 ppm) evidences a stronger association of **12**.

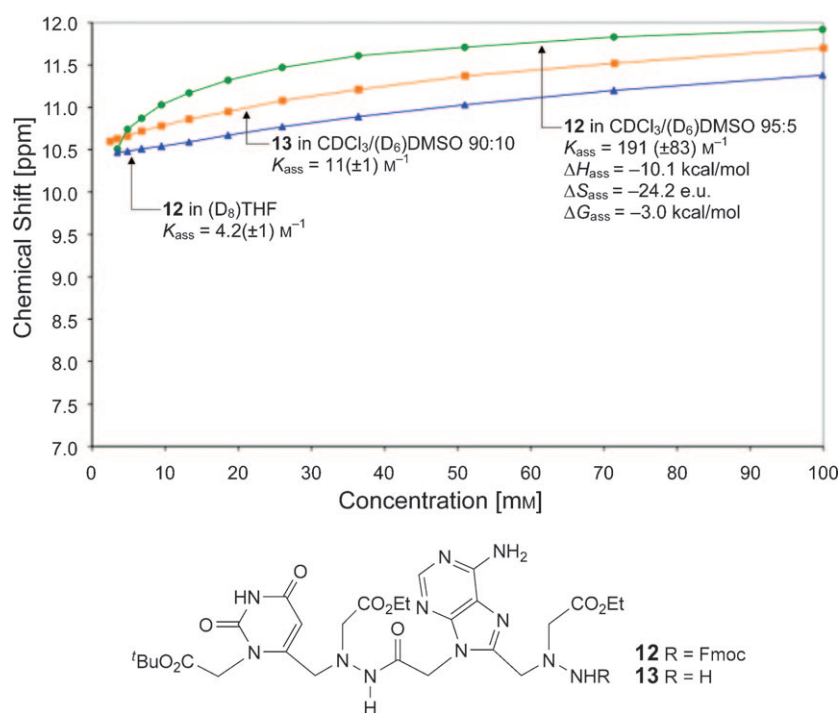


Fig. 4. SCCs for H–N(3) of the UA dimers **12** and **13** in $\text{CDCl}_3/(\text{D}_6)\text{DMSO}$ 95:5 and 90:10, and in $(\text{D}_8)\text{THF}$ (solid lines: fitted curve); values for the association constants and thermodynamic parameters of **12** in $\text{CDCl}_3/(\text{D}_6)\text{DMSO}$ 95:5

The sharpening of the $^1\text{H-NMR}$ signals of **12** upon addition of 5% DMSO suggests that the broad signals in CDCl_3 solution result from the formation of several types of associates (partially dissociating upon the addition of DMSO) and to equilibria of diastereoisomers resulting from the restricted rotation about the hydrazide and carbamate C–N bonds. $^1\text{H-NMR}$ Spectra in pure $(\text{D}_6)\text{DMSO}$ could not be used to detect if the hydrazides from (*E*)- and (*Z*)-isomers in the absence of pairing, as **12** degraded slowly, partial loss of the *N*Fmoc group being observed by TLC.

Two sets of signals for **12** were observed in $(\text{D}_8)\text{THF}$, in agreement with a mixture of (*E*)- and (*Z*)-isomers. The weak concentration dependence of $\delta(\text{H-N}(3))$ of **12** in $(\text{D}_8)\text{THF}$ (Fig. 4) resulted in an insignificant association constant of $4.2(\pm 1) \text{ M}^{-1}$.

The partially deprotected UA dimer **13** was insoluble in CDCl_3 and poorly soluble in $\text{CDCl}_3/(\text{D}_6)\text{DMSO}$ 95:5. A $^1\text{H-NMR}$ spectrum of a saturated solution of **13** in this solvent mixture (*ca.* 10 mM) showed broad signals, with the one of H–N(3) barely discernible between *ca.* 11.8 and *ca.* 11.0 ppm. In $\text{CDCl}_3/(\text{D}_6)\text{DMSO}$ 90:10, the $^1\text{H-NMR}$ spectrum of **13** displayed sufficiently sharp signals to determine the concentration dependence of $\delta(\text{H-N}(3))$ between 50 and 1 mM (Fig. 4), resulting in a very small association constant of $11(\pm 1) \text{ M}^{-1}$.

Self-Association of Hydrazide-Linked Tetranucleotide Analogues. The $^1\text{H-NMR}$ spectra of the *N*-Fmoc-protected U_4 tetramer **17** in CDCl_3 is characterized by strong signal broadening. We could only tentatively assign the broad signals, with the fluorenyl signals appearing as three broad peaks between 7.8 and 7.2 ppm, those of all CH_2 groups as a single, very broad peak at 4.6–3.2 ppm, and those of Me and *t*Bu groups as two broad peaks between 1.6 and 1.0 ppm. No other signals were detected. Similarly broad signals characterized the $^1\text{H-NMR}$ spectra of **17** in $\text{CDCl}_3/(\text{D}_6)\text{DMSO}$ 95:5, while sharper signals for solutions in $\text{CDCl}_3/(\text{D}_6)\text{DMSO}$ 90:10 allowed us to follow the concentration dependence of $\delta(\text{H-N}(3))$. The four H–N(3) of **17** (50 and 0.6 mM) resonate as a single, broad, concentration independent signal (Fig. 5). The chemical shift of 10.6–10.5 ppm is about the same as that for H–N(3) of the U monomer **41** (0.5 mM), evidencing that **17** does not associate in $\text{CDCl}_3/(\text{D}_6)\text{DMSO}$ 90:10.

The similar, concentration-independent chemical shift (10.5–10.4 ppm) of H–N(3) of **17** and of **41** (10.28 ppm) in $(\text{D}_8)\text{THF}$ at a concentration of 0.5 mM evidences that **17** does not associate in THF (Fig. 5).

Very similar results were obtained for the partially deprotected U_4 tetramer **18** in $\text{CDCl}_3/(\text{D}_6)\text{DMSO}$ 90:10, and in $(\text{D}_8)\text{THF}$ at concentrations between 25 and 1 mM. The insensitivity of $\delta(\text{H-N}(3))$ to the change of concentration evidences that **18** does not associate in these solvents. The tetramer **18** proved too poorly soluble in CDCl_3 to establish a SCC, and the spectra of saturated solutions in $\text{CDCl}_3/(\text{D}_6)\text{DMSO}$ 95:5 were too broad to be analysed.

Similarly, we could not derive a SCC for the self-complementary U- and A-derived tetramers **20** and **22** (Scheme 2). They proved too poorly soluble in CDCl_3 , $\text{CDCl}_3/(\text{D}_6)\text{DMSO}$ 95:5, and $(\text{D}_8)\text{THF}$, and the $^1\text{H-NMR}$ signals of solutions in $\text{CDCl}_3/(\text{D}_6)\text{DMSO}$ 90:10 were too broad. The spectra of **20** and **22** in $(\text{D}_6)\text{DMSO}$ (where no association is expected) are characterized by sharper, but complex signals.

In summary, the hydrazide-linked di- and tetramers do not pair in any of the solvents studied, in contradistinction to the formation of a cyclic duplex of the UU dimer **5** in the solid state. The signal splitting in the $^1\text{H-NMR}$ spectra in $(\text{D}_6)\text{DMSO}$ or

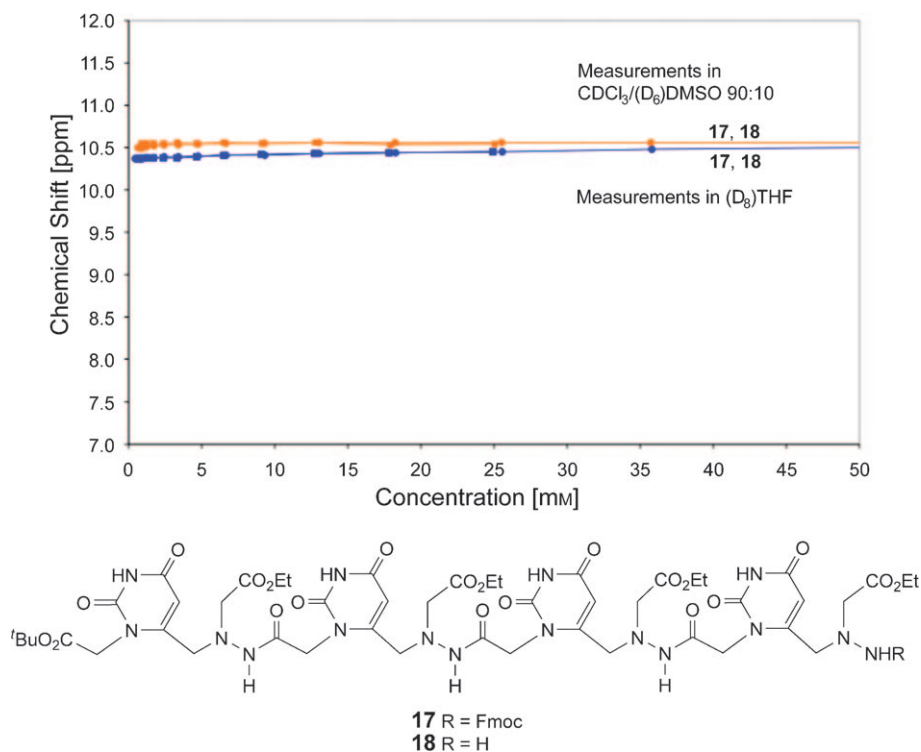


Fig. 5. SCCs for $H-N(3)$ of the U_4 tetramers **17** and **18** in $\text{CDCl}_3/(\text{D}_8)\text{DMSO}$ 90:10 and in $(\text{D}_8)\text{THF}$ (solid lines: fitted curve)

in $(\text{D}_8)\text{THF}$ evidences (*E*)- and (*Z*)-hydrazide isomers, and the broad $^1\text{H-NMR}$ signals in the less polar solvents or solvent mixtures suggest the formation of equilibrating linear associates.

Analysis of Association of the Hydrazide-Linked Octamers. We tested stacking of the self-complementary octamers **24**–**32** by monitoring the UV absorption of a $10\ \mu\text{M}$ solution in H_2O or in 10 mM Na-phosphate buffer at pH 7 at 260 nm, increasing the temperature from 4 to 80° in increments of $0.1^\circ/\text{min}$, and then cooling the solution to 4° [18]. We also recorded a UV melting curve of a mixture of **28** (U_2A_2)₂ and **30** (A_2U_2)₂ ($c = 5 + 5\ \mu\text{M}$), allowing for hetero-association with parallel strand orientation. The results from the heating and cooling experiments were identical. The absence of any hyper- or hypochromic effect for **24**–**32**, at 260, 270, 280, and 290 nm, and at concentrations of 10–100 mM shows the absence of any intra- or intermolecular stacking. This conclusion is confirmed by the ESI-MS of **30**, **31**, and **32** at a concentration of 1 mM, where only peaks of the singly or doubly charged monoplexes were detected.

The absence of stacking interactions suggests the absence of pairing. In addition to the unfavourable conformation for the formation of H-bonds between the nucleobases that may disfavour pairing of the hydrazide-linked di- and tetramers in organic solvents,

stacking in H₂O may be disfavoured by the calculated [2] large distance between the planes of the nucleobases (*cf.* hydrazide analogues: 3.6–4 Å; A-DNA and B-DNA: 3.3–3.4 Å) and the energetic penalty required for reducing it, considering the rather rigid linker. This penalty is expressed by the buckle twists in the crystal structure of **5** (*Fig. 1*), and visible in the energetically minimized octamer U₄A₄ in [2].

*Association of **33** with DNA and RNA.* To test for hetero-association of the hydrazide-linked U₁₀ decamer **33** with the complementary strands **43** of DNA and **42** of RNA (A₁₀), we monitored the UV absorption, while heating and cooling the solution of the mixtures **33/43** and **33/42** (*c* = 5 μM each; 10 mM Na-phosphate buffer: 100 mM NaCl and 0.1 mM EDTA, pH 7) between 4° and 80°. As a negative control, we recorded UV melting curves of the individual, non-self-complementary strands (*c* = 5 μM) in the same temperature range (*Fig. 6*).

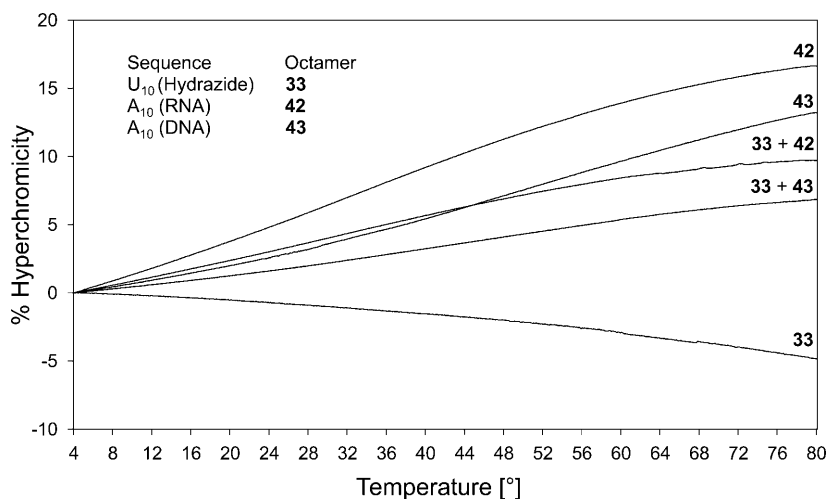


Fig. 6. Temperature dependence of the UV absorption of the decamers **33**, **43**, and **42**. Recorded in 10 mM Na-phosphate buffer (100 mM NaCl, 0.1 mM EDTA), *c* = 5 + 5 μM, *λ* = 260 nm, 1-cm cell.

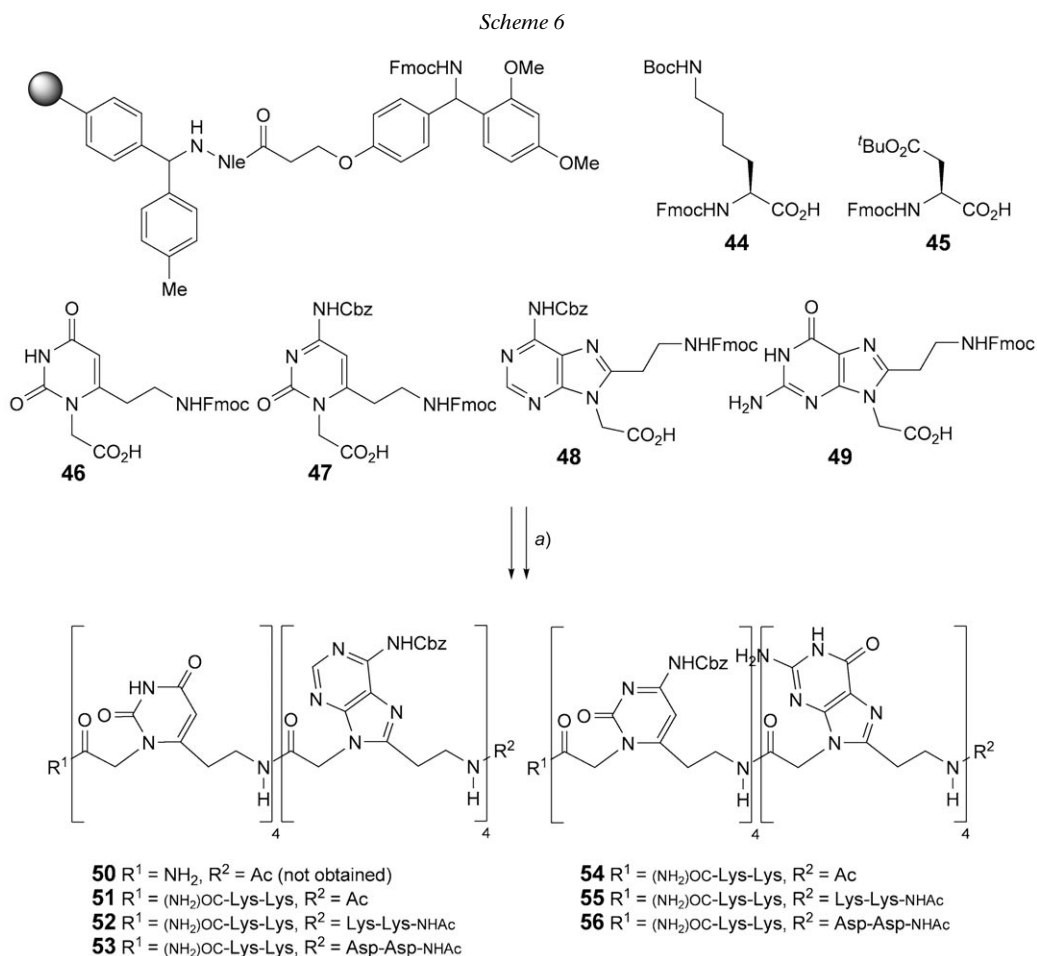
The smooth, not completely straight curves of the individual decamers **43**, **42**, and **33** indicate unspecific stacking. The curves for the mixtures **33/43** and **33/42** represent an overlap of the individual curves.

Considering that a sufficient degree of flexibility of the linker is crucial for the association into helical structures, we conclude that peptide-linked ONIBs require a longer linking element, comprising functional groups that allow for conformational changes and induce a conformation of the monoplex that favours pairing. Such peptide-linked ONIBs may lead to a large twist angle, and we intend to explore if such a large twist angle will allow for a sufficient degree of stacking to favour pairing.

Attempted Synthesis of Amide-Linked Octamers. We attempted to synthesize the self-complementary octamer **50** (U₄A^{Cbz}₄) on the *Rink* amide MBHA resin [22] under similar conditions as described for the synthesis of the hydrazide-linked octamers, but with the necessity of coupling the acids **46** and **48** twice at 35° for 8–10 h each time to

realize satisfactory coupling yields. In spite of this, we did not detect **50** by LC/MS analysis. This may well reflect a poor solubility of the product in H₂O, resulting from replacing an N-alkyl group of the hydrazides by a CH₂ group, and omitting the side chain. We, therefore, synthesized the octamers **51–56** (Scheme 6), modified at the N- and C-terminus by incorporation of lysine and aspartic acid residues, as lysine is well-known to increase the solubility of PNA oligomers in H₂O [34]. The amino acids were used in a fivefold excess and doubly coupled for 30 min.

The U-, A-, C-, and G-derived self-complementary benzyloxycarbonylated octamers **51–56** were isolated as the main products of the synthesis on a *Rink* amide MBHA resin, besides truncated sequences resulting from incomplete coupling of the purine-derived monomers (Scheme 6). However, debenzyloxycarbonylation of these



a) *Solid-Phase Synthesis*. Loading and coupling: *Rink* amide MBHA polystyrene resin, **46**, **47**, **48**, **49**, **44**, or **45**, HATU, *Hünig*'s base, DMSO. *N*-Fmoc deprotection: DBU, DMSO. Capping: Ac₂O, *Hünig*'s base, NMP. Cleavage from the resin: TFA/^tPr₃SiH 97:3.

octamers under hydrogenolytic or acidic conditions did not lead to the desired deprotected octamers, probably owing to their insolubility in aqueous solution.

We thank Dr. *Bruno Bernet* for checking the experimental data, Dr. *Bernd Schweizer* for the crystal structure analysis, and *Syngenta AG*, Basel, for generous support.

Experimental Part

General. THF was distilled from Na/benzophenone, and CH_2Cl_2 , MeOH, DMF, pyridine, $\text{Et}^{\text{N}}\text{Pr}_2$, and $^{\text{I}}\text{Pr}_2\text{NH}$ from CaH_2 . Reactions were run under N_2 . Qual. TLC: precoated silica-gel plates (*Merck* silica gel 60 F_{254}); detection by UV light at 254 nm wavelength and by spraying with 'mostain', and heating. Flash chromatography (FC): silica gel *Fluka 60* or *Merck 60* (0.04–0.063 mm). UV Spectra: 10^{-5} M solns. in CHCl_3 or MeOH at 20° in a 1-cm *Suprasil* cell. FT-IR: solid state (ATR). ^1H - and ^{13}C -NMR: at 300 or 400 MHz and 75 or 100 MHz, resp. MS: Matrix-assisted laser desorption ionization time-of-flight mass spectrometry (MALDI-TOF) with 0.05M indole-3-acrylic acid (IAA) in THF, or with 0.05M α -cyano-4-hydroxycinnamic acid (CCA) in MeCN/EtOH/ H_2O , and high-resolution (HR) MALDI-TOF with 0.05M 2,5-dihydrobenzoic acid (DHB) in THF.

General Procedure for Concentration- and Temperature-Dependent NMR Studies. NMR Experiments were performed at 295 K and at 300 MHz in CDCl_3 , 5% (D_6)DMSO/ CDCl_3 , 10% (D_6)DMSO/ CDCl_3 , or (D_8)THF (passed through basic aluminium oxide and dried over mol. sieves (4 Å) prior to use). Experiments started at the highest concentration, with stepwise replacement of 0.2 ml of the 0.7-ml soln. with 0.2 ml of solvent. The data were analysed by non-linear least-squares fitting using MATLAB (trust-region algorithm); the parameters were K_{ass} , $\delta(\text{H-N}(3))$, $c = 0$ mM, and $\delta(\text{H-N}(3))$, $c = \infty$. The thermodynamic parameters were determined by *van't Hoff* analysis. The uracil $\delta(\text{H-N}(3))$ was monitored at 7, 15, 22, 30, 40, and 50°, and at a fixed concentration of 10 mM.

General Procedure for Temperature-Dependent UV Spectroscopy. UV Experiments were performed by equilibrating 10 μM soln. of the oligomers in H_2O or in 10 mM Na-phosphate buffer (100 mM NaCl and 0.1 mM EDTA, pH 7) for 30 min at 4°, heating to 80°, and cooling the soln. back to 4° (rate of 0.1°/min). The required UV absorption at λ 260 nm to obtain 5 or 10 μM soln. was calculated by *Lambert-Beer's* law via the extinction coefficients of the oligomers, which were in turn calculated by summing up the extinction coefficients of the monomers ($U(T)$: 8.7, A : 15.4 ml/ μmol^{-1} cm^{-1}).

tert-Butyl 6- $\{[1-(2\text{-ethoxy-2-oxoethyl})-2-[(9\text{H-fluoren-9-yl)methoxycarbonyl]hydrazino]methyl\}$ uracil-1-acetyl- ($I^2 \rightarrow 6^3\text{-N}$)-6- $\{[1-(2\text{-ethoxy-2-oxoethyl})hydrazino]methyl\}$ uracil-1-acetate (= (9H-Fluoren-9-yl)methyl 2- $\{[3-[2-[2-((3-[2-(tert\text{-Butoxy})-2\text{-oxoethyl}]-2,6\text{-dioxo-1,2,3,6-tetrahydropyrimidin-4-yl)-methyl]-2-(2\text{-ethoxy-2-oxoethyl})hydrazinyl]-2\text{-oxoethyl}]-2,6\text{-dioxo-1,2,3,6-tetrahydropyrimidin-4-yl)-methyl]-2-(2\text{-ethoxy-2-oxoethyl})hydrazinecarboxylate$; **5**). A soln. of **4** (3.9 g, 7.5 mmol) in DMF (120 ml) was cooled to 0°, treated with HOBt (1.1 g, 8.1 mmol) and HBTU (3.2 g, 8.4 mmol), stirred for 1.5 h at r.t., treated with a soln. of **3** (2.5 g, 7.0 mmol) in DMF (25 ml) and with $\text{Et}^{\text{N}}\text{Pr}_2$ (1.5 ml, 8.6 mmol), stirred for 20 h, treated with sat. NaHCO_3 soln. (150 ml), and extracted with AcOEt (5×150 ml). Drying of the combined org. layers (MgSO_4), filtration, evaporation, and FC ($\text{CH}_2\text{Cl}_2/\text{MeOH}$ 97:3 \rightarrow 90:10) gave **5** (5.95 g, 98%). White powder. R_f ($\text{CH}_2\text{Cl}_2/\text{MeOH}$ 9:1) 0.54. M.p. (of a small batch crystallized from EtOH) 130–132°. UV (CHCl_3): 267 (35600), 301 (5300). IR (ATR): 3224w (br.), 2980w, 1675s (br.), 1627m, 1451m, 1421m, 1389m, 1228m, 1204m, 1153s, 1072w, 1024w, 980w, 930w, 822w. ^1H -NMR (400 MHz, (D_6)DMSO; ca. 2:1 mixture of rotamers; assignments based on a DQFCOSY, a HSQC, and a HMBC spectrum): 11.39 (0.6 H), 11.34 (0.6 H), 11.29 (0.8 H) (3s, 2 H-N(3)); 9.66 (0.4 H), 8.90 (0.6 H) (2s, HN-NCH₂C(6I)); 8.85 (s, HN-NCH₂C(6II)); 7.88–7.30 (m, 8 arom. H); 5.63 (s, 0.7 H-C(5I)); 5.57 (s, 0.9 H-C(5II)); 5.52 (s, 0.3 H-C(5I)), 0.1 H-C(5II)); 5.31 (br. d, $J = 17.2$, 0.2 CH₂-N(1II)); 5.22 (br. d, $J = 17.2$, 0.2 CH₂-N(1I)); 4.94 (s, 0.6 CH₂-N(1I)); 4.81 (br. s, 0.5 CH₂-N(1II)); 4.71 (br. d, $J = 17.2$, 0.3 CH₂-N(1II)); 4.60 (br. d, $J = 17.2$, 0.2 CH₂-N(1I)); 4.27 (br. s, CH₂-C(9)); 4.18 (br. s, H-C(9)); 4.08–4.05 (m, 2 MeCH₂O); 3.98 (br. s, 0.3 H); 3.80 (br. s, CH₂-C(6I)); 3.76 (br. s, CH₂NCH₂C(6I)); 3.73, 3.69 (2 br. s, CH₂-C(6II), CH₂NCH₂C(6II)); 3.56 (br. s, 0.3 H); 3.52 (br. s, 0.3 H); 1.43 (3 H), 1.39 (6 H) (2s, *t*-Bu); 1.20–1.11 (m, 2 MeCH₂O). ^{13}C -NMR (100 MHz, (D_6)DMSO; ca. 2:1 mixture of

rotamers; assignments based on a HSQC and a HMBC spectrum): signals of the major rotamer: 169.22, 169.05 (2s, 2 CO₂Et); 168.10 (s, CO₂Bu); 166.95 (s, C(O)CH₂N(1/II)); 81.52 (s, Me₃C); signals of the minor rotamer: 170.23 (s, C(O)CH₂N(1/II)); 169.36, 169.31 (2s, 2 CO₂Et); 167.94 (s, CO₂Bu); 81.67 (s, Me₃C); signals of both rotamers: 162.51, 162.47 (2s, 2 C(4)); 155.22 (br. s, NCO₂); 151.70, 151.63, 151.60, 151.22, 149.75 (5s, 2 C(2), C(6/II)); 150.69 (s, C(6/I)); 143.62 (2 br. s); 140.71 (2 br. s); 127.66 (2 br. d); 127.10 (2 br. d); 125.08 (2 br. d); 120.08 (2 br. d); 105.33, 103.86, 103.77, 103.39 (4d, 2 C(5)); 65.68 (t, CH₂-C(9')); 60.49, 60.36, 60.32, 60.26, 59.25 (5t, 2 MeCH₂O, CH₂NCH₂C(6/II)); 57.51 (br. t, CH₂-C(6/II)); 56.54 (t, CH₂NCH₂C(6/I)); 56.41 (t, CH₂-C(6/I)); 46.58 (d, C(9')); 45.21 (t, CH₂-N(1/I)); 44.03 (t, CH₂-N(1/II)); 27.59 (q, Me₃C); 13.99, 13.94, 13.85 (3q, 2 MeCH₂O). HR-MALDI-MS: 883.3248 (100, [M + Na]⁺, C₄₁H₄₈N₈NaO₁₃; calc. 883.3233), 827.2614 (41, [M - 'Bu + H + Na]⁺, C₃₇H₄₀N₈NaO₁₃; calc. 827.2602), 805.2819 (75, [M - 'Bu + 2 H]⁺, C₃₇H₄₁N₈O₁₃; calc. 805.2782), 583.2117 (30, [M - 'Bu - Fmoc + 3 H]⁺, C₂₂H₃₁N₈O₁₁; calc. 583.2101). Anal. calc. for C₄₁H₄₈N₈O₁₃·CH₄O (892.91): C 56.50, H 5.87, N 12.55; found: C 56.70, H 5.76, N 12.69.

Crystal Structure Analysis of 5. Crystals of **5** were obtained by slow evaporation of a soln. of **5** in EtOH (dimensions of the analysed crystal: cube 0.3 × 0.2 × 0.1 mm). C₄₁H₄₈N₈O₁₃·C₂H₆O·H₂O, *M_r* 924.96, triclinic *P*1̄, *a* = 14.0050(3), *b* = 14.0670(3), *c* = 15.0703(4) Å, *α* = 63.6474(11), *β* = 72.1477(10), *γ* = 61.3441(12)°, *V* = 2317.94(9) Å³, *Z* = 2, *D_x* = 1.325 Mg m⁻³. The reflections were measured on a *Kappa*CCD diffractometer, with MoK_α radiation, *λ* = 0.71073 Å. Cell parameters from 32355 refl., *θ* = 2.425–27.485°, *μ* = 0.101 mm⁻¹, *T* = 203 K. 18629 measured reflections; 10576 independent reflections; 7455 observed reflections (> 2σ(*I*)). Refinement on *F*²: full-matrix least-squares refinement, *R*(all) = 0.1096, *R*(gt) = 0.0804. All diagrams and calculations were performed using *maxUs* (Bruker Nonius, Delft & MacScience, Japan). The program SIR97 was used to solve the structure and the program SHELXL-97 to refine it.

tert-Butyl 6-[[1-(2-Ethoxy-2-oxoethyl)hydrazino]methyl]uracil-1-acetyl-(1² → 6³-N)-6-[[1-(2-ethoxy-2-oxoethyl)hydrazino]methyl]uracil-1-acetate (= Ethyl (1-((3-[2-(tert-Butoxy)-2-oxoethyl]-2,6-dioxo-1,2,3,6-tetrahydropyrimidin-4-yl)methyl)-2-[[6-[[1-(2-ethoxy-2-oxoethyl)hydrazinyl]methyl]-2,4-dioxo-3,4-dihydropyrimidin-1(2H)-yl]acetyl]hydrazinyl)acetate; **6**). A soln. of **5** (1 g, 1.2 mmol) in DMF (10 ml) was treated dropwise with piperidine (0.6 ml, 6.1 mmol), stirred for 2 h at r.t., and evaporated. The solid residue was washed with Et₂O (8 × 10 ml). The solid was suspended in CH₂Cl₂ (100 ml) and filtered. Evaporation of the filtrate gave **6** (0.74 g, 99%). White powder. *R_f* (CH₂Cl₂/MeOH 9:1) 0.22. *M.p.* 153–157°. UV (CHCl₃): 266 (19600). IR (ATR): 3200w (br.), 2981w, 2808w, 1673s (br.), 1461m, 1419m, 1389m, 1370m, 1294w, 1235m, 1200m, 1154s, 1074w, 1024w, 980w, 927w, 819m. ¹H-NMR (400 MHz, (D₆)DMSO; *ca.* 2:1 mixture of rotamers; assignments based on a DQFCOSY, a HSQC, and a HMBC spectrum): 11.29 (br. s, 2 H-N(3)); 9.55 (0.6 H), 8.89 (0.4 H) (2s, HN-NCH₂C(6/I)); 5.61 (s, 0.7 H-C(5/I)); 5.58, 5.57 (2s, 0.7 H-C(5/II), 0.3 H-C(5/I)); 5.54 (s, 0.3 H-C(5/II)); 5.07 (br. d, *J* = 17.2, 0.2 CH₂-N(1/I)); 5.03 (br. d, *J* = 17.2, 0.2 CH₂-N(1/II)); 4.90 (s, 0.6 CH₂-N(1/I)); 4.60–4.53 (m, 0.8 CH₂-N(1/II), 0.2 CH₂-N(1/I)); 4.14, 4.10, 4.08 (3q, *J* = 7.1, 2 MeCH₂O); 3.92 (s, 0.1 H); 3.88 (s, 0.3 H); 3.83 (s, 0.4 H); 3.80 (s, CH₂-C(6/I)); 3.77 (s, CH₂NCH₂C(6/I)); 3.73 (br. s, NH₂); 3.59 (s, 0.3 H); 3.56 (s, 0.4 H); 3.51 (s, CH₂-C(6/II)); 3.48, 3.47, 3.46 (3s, 0.9 H); 3.44 (s, CH₂NCH₂C(6/II)); 3.43 (s, 0.2 H); 1.43 (3 H), 1.39 (6 H) (2s, *t*-Bu); 1.23–1.18 (m, 2 MeCH₂O). ¹³C-NMR (100 MHz, (D₆)DMSO; *ca.* 2:1 mixture of rotamers; assignments based on a HSQC and a HMBC spectrum): signals of the major rotamer: 169.93 (s, C(O)CH₂NCH₂C(6/II)); 169.27 (s, C(O)CH₂NCH₂C(6/I)); 168.03 (s, CO₂Bu); 166.70 (s, C(O)CH₂N(1/II)); 162.69 (s, C(4/II)); 162.48 (s, C(4/I)); 152.10 (s, C(6/II)); 151.81, 151.67 (2s, 2 C(2)); 150.76 (s, C(6/I)); 81.55 (s, Me₃C); 60.38 (t, CH₂-C(6/II)); 56.54 (t, CH₂NCH₂C(6/I)); 56.27 (t, CH₂-C(6/I)); 27.60 (q, Me₃C); signals of the minor rotamer: 170.11 (s, CO₂Et); 169.98 (s, C(O)CH₂N(1/II)); 167.72 (s, CO₂Bu); 162.74 (s, C(4/II)); 162.44 (s, C(4/I)); 152.60 (s, C(6/II)); 151.77, 151.61 (2s, 2 C(2)); 149.74 (s, C(6/I)); 81.81 (s, Me₃C); 57.59 (br. t, CH₂-C(6/I)); 27.63 (q, Me₃C); signals of both rotamers: 103.72 (d, 2 C(5)); 60.62, 60.34, 60.23, 60.17, 60.02, 59.97, 59.93, 59.20 (8t, 2 MeCH₂O, 2 CH₂NCH₂C(6), CH₂-C(6/II)); 45.22 (t, CH₂-N(1/I)); 43.94 (t, CH₂-N(1/II)); 14.05, 13.96 (2q, 2 MeCH₂O). HR-MALDI-MS: 661.2541 (44, [M + Na]⁺, C₂₆H₃₈N₈NaO₁₁; calc. 661.2552), 639.2733 (33, [M + H]⁺, C₂₆H₃₉N₈O₁₁; calc. 639.2733), 605.1911 (16, [M - 'Bu + H + Na]⁺, C₂₂H₃₀N₈NaO₁₁; calc. 605.1921), 583.2101 (100, [M - 'Bu + 2 H]⁺, C₂₂H₃₁N₈O₁₁; calc. 583.2101).

122.55 (s, C(5/II)); 105.32 (d, C(5/I)); 82.00 (s, Me₃C); 61.36, 61.32 (2t, 2 MeCH₂O); 57.77 (t, CH₂NCH₂C(8/II)); 56.96 (t, CH₂NCH₂C(6/I)); 56.70 (t, CH₂-C(6/I)); 54.30 (t, CH₂-C(8/II)); 46.19 (t, CH₂-N(1/I)); 44.70 (t, CH₂-N(9/II)); signals of the minor rotamer: 170.99, 170.25 (2s, 2 CO₂Et); 168.95 (s, CO₂Bu); 162.83 (s, C(4/I)); 156.66 (s, N-NCO₂); 154.78 (s, C(4/II)); 152.86 (d, C(2/II)); 152.40, 151.73 (2s, C(2/I), C(6/I), NCO₂-C(6/II)); 122.47 (s, C(5/II)); 106.54 (d, C(5/I)); 82.33 (s, Me₃C); 61.55 (t, MeCH₂O); 59.53, 59.15, 54.70 (3t, CH₂NCH₂C(8/II), CH₂NCH₂C(6/I), CH₂-C(8/II)); 57.23 (t, CH₂-C(6/I)); 46.27 (t, CH₂-N(1/I)); 44.46 (t, CH₂-N(9/II)); signals of both rotamers: 150.19, 149.99 (2s, C(6/II), C(8/II)); 145.01 (2s); 142.18 (2s); 137.75 (s); 129.04 (2d); 128.89 (2d); 128.58 (d); 128.29 (2d); 127.73 (2d); 125.99 (2d); 120.51 (2d); 66.95 (t, PhCH₂, CH₂-C(9')); 48.06 (d, C(9')); 28.19 (q, Me₃C); 14.48 (q, 2 MeCH₂O). HR-MALDI-MS: 1040.3892 (100, [M + Na]⁺, C₅₀H₅₅N₁₁NaO₁₃; calc. 1040.3873), 1018.4082 (59, [M + H]⁺, C₅₀H₅₆N₁₁O₁₃; calc. 1018.4054).

6-[[1-(2-Ethoxy-2-oxoethyl)-2-acetylhydrazino]methyl]uracil-1-acetyl-[(1² → 6³-N)-6-[[1-(2-ethoxy-2-oxoethyl)hydrazino]methyl]uracil-1-acetyl]₈-(1² → 6³-N)-6-[[1-(2-ethoxy-2-oxoethyl)hydrazino]methyl]uracil-9-acetamid (= Ethyl [1-[[6-[[[(Benzyl)oxy]carbonyl]amino]-9-[2-[2-[[3-[2-(tert-butoxy)-2-oxoethyl]-2,6-dioxo-1,2,3,6-tetrahydropyrimidin-4-yl]methyl]-2-(2-ethoxy-2-oxoethyl)hydrazinyl]-2-oxoethyl]-9H-purin-8-yl]methyl]hydrazinyl]acetate; **10**). A soln. of **9** (800 mg, 0.8 mmol) in DMF (10 ml) was treated dropwise with piperidine (0.8 ml, 7.9 mmol), stirred for 3.5 h at r.t., and evaporated. MPLC (CH₂Cl₂/MeOH 93 : 7, flow: 30 ml/min) gave **10** (503 mg, 80%). White powder. R_f (CH₂Cl₂/MeOH 9 : 1) 0.50. M.p. 104–108°. UV (CHCl₃): 270 (27730). IR (ATR): 3196w (br.), 2979w, 2931w, 1734s, 1687s, 1613m, 1590m, 1535w, 1498w, 1454m, 1424m, 1391m, 1369m, 1321w, 1296w, 1232m, 1201s, 1155s, 1099m, 1027m, 976w, 863w, 820w. ¹H-NMR (400 MHz, (D₈)THF; ca. 4 : 1 mixture of rotamers; assignments based on a HSQC and a HMBC spectrum): 10.44 (br. s, H-N(3/I)); 9.64 (0.8 H), 9.56 (0.2 H) (2 br. s, HN-C(6/II)); 8.97 (0.8 H), 8.27 (0.2 H) (2s, HN-NCH₂C(6/I)); 8.50 (0.8 H), 8.45 (0.2 H) (2s, H-C(2/II)); 7.46–7.23 (m, 5 arom. H); 5.64 (0.2 H), 5.57 (0.8 H) (2s, H-C(5/I)); 5.57 (0.2 H), 5.26 (0.3 H), 5.04 (0.3 H), 4.84 (0.2 H) (4 br. d, J = 17.4, 0.5 CH₂-N(1/I), 0.5 CH₂-N(9/II)); 5.23 (s, PhCH₂); 5.12 (s, 0.5 CH₂-N(9/II)); 4.90 (s, 0.5 CH₂-N(1/I)); 4.19 (s, CH₂-C(8/II)); 4.14, 4.13 (2q, J = 7.2, 2 MeCH₂O); 3.97 (s, CH₂-C(6/I)); 3.93 (0.4 H); 3.88 (s, CH₂NCH₂C(6/I)); 3.55 (s, CH₂NCH₂C(8/II)); 3.50 (0.4 H); 1.46 (2 H), 1.37 (7 H) (2s, *t*-Bu); 1.23 (t, J = 7.2, 2 MeCH₂O). ¹³C-NMR (100 MHz, (D₈)THF; assignments based on a HSQC and a HMBC spectrum): 171.09 (s, C(O)CH₂NCH₂C(8/II)); 170.57 (s, C(O)CH₂NCH₂C(6/I)); 169.31 (s, CO₂Bu); 167.44 (s, C(O)CH₂N(9/II)); 163.03 (s, C(4/I)); 154.75 (s, C(4/II)); 152.75 (s, C(8/II)); 152.66 (s, C(2/I)); 152.40 (s, NCO₂); 152.26 (d, C(2/II)); 151.32 (s, C(6/I)); 150.08 (s, C(6/II)); 137.82 (s); 129.04 (2d); 128.88 (2d); 128.56 (d); 122.74 (s, C(5/II)); 105.21 (d, C(5/I)); 82.04 (s, Me₃C); 66.94 (t, PhCH₂); 61.33, 60.85 (2t, 2 MeCH₂O); 60.97 (t, CH₂NCH₂C(8/II)); 58.48 (t, CH₂-C(8/II)); 56.91 (t, CH₂NCH₂C(6/I)); 56.49 (t, CH₂-C(6/I)); 46.18 (t, CH₂-N(1/I)); 44.56 (t, CH₂-N(9/II)); 28.16 (q, Me₃C); 14.52, 14.44 (2q, 2 MeCH₂O). HR-MALDI-MS: 818.3170 (39, [M + Na]⁺, C₃₅H₄₅N₁₁NaO₁₁; calc. 818.3192), 796.3366 (100, [M + H]⁺, C₃₅H₄₆N₁₁O₁₁; calc. 796.3373).

8-[[1-(2-Ethoxy-2-oxoethyl)-2-[(9H-fluoren-9-yl)methoxycarbonyl]hydrazino]methyl]-N⁶-(benzyl-oxycarbonyl)adenine-9-acetyl-(9² → 6³-N)-6-[[1-(2-ethoxy-2-oxoethyl)hydrazino]methyl]uracil-1-acetic Acid (= [6-[[2-[[6-[[[(Benzyl)oxy]carbonyl]amino]-8-[[1-(2-ethoxy-2-oxoethyl)-2-[(9H-fluoren-9-yl)methoxy]carbonyl]hydrazinyl]methyl]-9H-purin-9-yl]acetyl]-1-(2-ethoxy-2-oxoethyl)hydrazinyl]methyl]-2,4-dioxo-3,4-dihydropyrimidin-1(2H)-yl]acetic Acid; **11**). A soln. of **9** (800 mg, 0.8 mmol) in CH₂Cl₂ (10 ml) was treated with Et₃SiH (0.2 ml, 1.2 mmol) and TFA (1.75 ml, 23.6 mmol), stirred for 3 h at r.t., and evaporated. MPLC (CH₂Cl₂/MeOH 90 : 10 → 80 : 20, flow: 30 ml/min) gave **11** (684 mg, 84%). White powder. R_f (AcOEt/MeOH/H₂O 7 : 2 : 1) 0.50. M.p. > 139° (dec.). UV (CHCl₃): 269 (42500), 301 (5200). IR (ATR): 3510–2330w (br.), 3208w (br.), 2982w, 1682s (br.), 1613m, 1530w, 1495w, 1451m, 1416m, 1392m, 1322w, 1202s, 1166s, 1103m, 1027m, 826m. ¹H-NMR (500 MHz, (D₈)THF; ca. 2 : 1 mixture of rotamers; assignments based on a HSQC and a HMBC spectrum): 10.60 (0.3 H), 10.46 (0.7 H) (2s, H-N(3/I)); 9.61 (br. s, HN-C(6/II)); 9.21 (0.7 H), 8.28 (0.3 H) (2s, HN-NCH₂C(6/I)); 8.51 (0.7 H), 8.48 (0.3 H) (2s, H-C(2/II)); 8.21 (br. s, HN-NCH₂C(8/II)); 7.74–7.16 (m, 13 arom. H); 5.94, 5.48 (2 br. d, J = 17.0, 0.25 CH₂-N(1/I), 0.25 CH₂-N(9/II)); 5.64 (0.3 H), 5.58 (0.7 H) (2s, H-C(5/I)); 5.34 (br. s, 0.5 CH₂-N(9/II)); 5.17 (s, PhCH₂); 5.02 (s, 0.25 CH₂-N(1/I), 0.25 CH₂-N(9/II)); 5.00 (s, 0.5 CH₂-N(1/I)); 4.46 (br. s, CH₂-C(8/II)); 4.28 (0.6 H), 4.22 (1.4 H) (2d, J = 7.5, CH₂-C(9')); 4.19–4.09 (m, 2 MeCH₂O, H-C(9')); 4.01 (s, CH₂-C(6/I)); 4.00 (br. s, 0.5 H); 3.88 (s, CH₂NCH₂C(6/I)); 3.81 (br. s,

$\text{CH}_2\text{NCH}_2\text{C}(8/\text{II})$); 3.72 (s, 0.7 H); 1.24–1.16 (m, 2 MeCH_2O). ^{13}C -NMR (125 MHz, (D_8) THF; ca. 2 : 1 mixture of rotamers; assignments based on a HSQC and a HMBC spectrum): signals of the major rotamer: 171.01, 170.39 (2s, 2 CO_2Et); 163.13 (s, C(4/I)); 156.53 (s, N– NCO_2); 154.60 (s, C(4/II)); 150.15 (s, C(6/II)); 145.00 (2s); 142.14 (2s); 137.73 (s); 129.03 (2d); 128.90 (2d); 128.56 (d); 128.26 (2d); 127.72 (2d); 126.00 (2d); 122.43 (s, C(5/II)); 120.48 (2d); 61.34, 61.26 (2t, 2 MeCH_2O); 56.82 (t, $\text{CH}_2\text{--C}(6/\text{I})$); 54.11 (t, $\text{CH}_2\text{--C}(8/\text{II})$); 48.02 (d, C(9')); signals of the minor rotamer: 167.69 (s, C(O) $\text{CH}_2\text{N}(9/\text{II})$); 162.98 (s, C(4/I)); 156.59 (s, N– NCO_2); 154.70 (s, C(4/II)); 149.98 (s, C(6/II)); 145.00 (2s); 142.17 (2s); 137.78 (s); 129.01 (2d); 128.86 (2d); 128.51 (d); 128.31 (2d); 127.72 (2d); 125.96 (2d); 122.40 (s, C(5/II)); 120.52 (2d); 61.51, 61.30 (2t, 2 MeCH_2O); 58.96 (t, $\text{CH}_2\text{--C}(6/\text{I})$); 54.46 (t, $\text{CH}_2\text{--C}(8/\text{II})$); 48.09 (d, C(9')); signals of both rotamers: 170.93, 170.73, 170.60, 170.52, 170.43 (5s, 2 CO_2Et , CO_2H , C(O) $\text{CH}_2\text{N}(9/\text{II})$); 152.94 (d, C(2/II)); 152.87; 152.70 (s, C(2/I)); 152.28 (s, C(6/II)– NCO_2); 151.43, 151.40 (2s, C(6/I), C(8/II)); 105.22 (d, C(5/I)); 67.03 (t, PhCH_2 , $\text{CH}_2\text{--C}(9')$); 57.71 (br. t, $\text{CH}_2\text{NCH}_2\text{C}(8/\text{II})$); 56.82 (t, $\text{CH}_2\text{NCH}_2\text{C}(6/\text{I})$); 45.25 (t, $\text{CH}_2\text{--N}(1/\text{I})$); 44.76 (t, $\text{CH}_2\text{--N}(9/\text{II})$); 14.47, 14.46 (2q, 2 MeCH_2O). HR-MALDI-MS: 984.3229 (100, $[\text{M} + \text{Na}]^+$, $\text{C}_{46}\text{H}_{47}\text{N}_{11}\text{NaO}_{13}^+$; calc. 984.3247), 962.3368 (86, $[\text{M} + \text{H}]^+$, $\text{C}_{46}\text{H}_{48}\text{N}_{11}\text{O}_{13}^+$; calc. 962.3428), 876.2634 (29, $[\text{M} - \text{BnOH} + \text{Na}]^+$, $\text{C}_{39}\text{H}_{39}\text{N}_{11}\text{NaO}_{12}^+$; calc. 876.2672), 854.2862 (34, $[\text{M} - \text{BnOH} + \text{H}]^+$, $\text{C}_{39}\text{H}_{40}\text{N}_{11}\text{O}_{12}^+$; calc. 854.2858).

tert-Butyl 8- $\{[1-(2\text{-Ethoxy-2-oxoethyl})-2-[(9\text{H-fluoren-9-yl)methoxycarbonyl}]hydrazino\}methyl\}$ -adenine-9-acetyl-(9 \rightarrow 6 \rightarrow 3-N)-6- $\{[1-(2\text{-ethoxy-2-oxoethyl})hydrazino\}methyl\}uracil-1\text{-acetate}$ (= (9H-Fluoren-9-yl)methyl 2- $\{[6\text{-Amino-9-}[2-[(3- $\{2\text{-tert-butoxy-2-oxoethyl}\}$]-2,6-dioxo-1,2,3,6-tetrahydropyrimidin-4-yl)methyl]-2-(2-ethoxy-2-oxoethyl)hydrazinyl]-2-oxoethyl]-9H-purin-8-yl)methyl]-2-(2-ethoxy-2-oxoethyl)hydrazinecarboxylate; **12**). A suspension of $\text{Pd}(\text{OAc})_2$ (110 mg, 0.5 mmol) in $\text{MeOH}/\text{CH}_2\text{Cl}_2$ 1 : 1 (5 ml) was stirred under H_2 for 1 h at r.t., treated with a soln. of **9** (500 mg, 0.5 mmol) in $\text{MeOH}/\text{CH}_2\text{Cl}_2$ 1 : 1 (10 ml), stirred for 30 h, and filtered through *Celite*. Evaporation of the filtrate and MPLC ($\text{CH}_2\text{Cl}_2/\text{MeOH}$ 93 : 7, flow: 25 ml/min) gave **12** (410 mg, 94%). White powder. R_f ($\text{CH}_2\text{Cl}_2/\text{MeOH}$ 9 : 1) 0.38. M.p. > 143 $^\circ$ (dec.). UV (CHCl_3): 267 (35600), 301 (5000). IR (ATR): 3406w, 3323w, 3270w, 3230w, 3192w (br.), 2977w, 1735s, 1691s, 1666s, 1651s, 1607m, 1582w, 1535w, 1465m, 1436m, 1398m, 1372m, 1325m, 1275m, 1248m, 1232m, 1206s, 1145s, 1079w, 1053w, 1026m, 961w, 944w, 904w, 858w, 836w, 816w.$

^1H -NMR (400 MHz, (D_8) THF; ca. 3 : 1 mixture of rotamers; assignments based on a HSQC and a HMBC spectrum): 10.76 (0.3 H), 10.54 (0.7 H) (2 br. s, H–N(3/I)); 9.02 (br. s, HN– $\text{NCH}_2\text{C}(6/\text{I})$); 8.15 (br. s, HN– $\text{NCH}_2\text{C}(8/\text{II})$); 8.10 (s, H–C(2/II)); 7.76–7.19 (m, 8 arom. H); 6.45 (br. s, NH_2); 5.82 (0.2 H), 5.40 (0.2 H), 5.14 (0.3 H), 4.91 (0.3 H) (4 br. d, $J = 17.4$, 0.5 $\text{CH}_2\text{--N}(1/\text{I})$, 0.5 $\text{CH}_2\text{--N}(9/\text{II})$); 5.58 (0.3 H), 5.56 (0.7 H) (2s, H–C(5/I)); 5.21 (br. s, 0.5 $\text{CH}_2\text{--N}(9/\text{II})$); 4.97 (s, 0.5 $\text{CH}_2\text{--N}(1/\text{I})$); 4.38 (br. s, $\text{CH}_2\text{--C}(8/\text{II})$); 4.29 (0.6 H), 4.23 (1.4 H) (2d, $J = 7.0$, $\text{CH}_2\text{--C}(9')$); 4.21–4.08 (m, 2 MeCH_2O , H–C(9')); 4.05 (br. s, 0.2 H); 4.00 (br. s, 0.3 H); 3.97 (s, $\text{CH}_2\text{--C}(6/\text{I})$); 3.86 (s, $\text{CH}_2\text{NCH}_2\text{C}(6/\text{I})$); 3.77 (br. s, $\text{CH}_2\text{NCH}_2\text{C}(8/\text{II})$); 3.67, 3.66, 3.65 (3 br. s, 0.6 H); 1.46 (2 H), 1.38 (7 H) (2s, *t*-Bu); 1.25–1.15 (m, 2 MeCH_2O). ^{13}C -NMR (100 MHz, (D_8) THF; ca. 4 : 1 mixture of rotamers; assignments based on a HSQC and a HMBC spectrum): signals of the major rotamer: 170.69, 170.51 (2s, 2 CO_2Et); 169.36 (s, CO_2tBu); 163.08 (s, C(4/I)); 156.78 (s, C(6/II)); 156.51 (s, N– NCO_2); 148.19 (s, C(8/II)); 145.08 (2s); 142.18 (2s); 128.26 (2d); 127.76 (2d); 126.07 (2d); 120.49 (2d); 119.18 (s, C(5/II)); 105.33 (d, C(5/I)); 81.96 (s, Me_3C); 61.26 (t, 2 MeCH_2O); 56.89 (t, $\text{CH}_2\text{NCH}_2\text{C}(6/\text{I})$); 56.69 (t, $\text{CH}_2\text{--C}(6/\text{I})$); 48.09 (d, C(9')); 46.20 (t, $\text{CH}_2\text{--N}(1/\text{I})$); 44.63 (t, $\text{CH}_2\text{--N}(9/\text{II})$); 28.19 (q, Me_3C); signals of the minor rotamer: 170.92, 170.58 (2s, 2 CO_2Et); 169.00 (s, CO_2tBu); 163.03 (s, C(4/I)); 156.67, 156.57 (2s, C(6/II), N– NCO_2); 150.28 (s); 148.59 (s, C(8/II)); 145.05 (2s); 142.20 (2s); 128.32 (2d); 127.76 (2d); 125.99 (2d); 120.54 (2d); 119.01 (s, C(5/II)); 106.35 (d, C(5/I)); 82.25 (s, Me_3C); 61.49, 61.19 (2t, 2 MeCH_2O); 59.31 (t); 59.07 (t); 54.72 (t); 48.16 (d, C(9')); 46.36 (t, $\text{CH}_2\text{--N}(1/\text{I})$); 44.13 (t, $\text{CH}_2\text{--N}(9/\text{II})$); 28.23 (q, Me_3C); signals of both rotamers: 167.96 (s, C(O) $\text{CH}_2\text{N}(9/\text{II})$); 153.87 (d, C(2/II)); 152.75 (s, C(2/I), C(4/II)); 151.33 (s, C(6/I)); 66.94 (t, $\text{CH}_2\text{--C}(9')$); 57.43 (br. t, $\text{CH}_2\text{NCH}_2\text{C}(8/\text{II})$); 54.18 (br. t, $\text{CH}_2\text{--C}(8/\text{II})$); 14.49, 14.45 (2q, 2 MeCH_2O). HR-MALDI-MS: 906.3488 (100, $[\text{M} + \text{Na}]^+$, $\text{C}_{42}\text{H}_{49}\text{N}_{11}\text{NaO}_{11}^+$; calc. 906.3505), 884.3661 (88, $[\text{M} + \text{H}]^+$, $\text{C}_{42}\text{H}_{50}\text{N}_{11}\text{O}_{11}^+$; calc. 884.3686), 850.2872 (12, $[\text{M} - \text{tBu} + \text{H} + \text{Na}]^+$, $\text{C}_{38}\text{H}_{41}\text{N}_{11}\text{NaO}_{11}^+$; calc. 850.2874), 828.3036 (24, $[\text{M} - \text{tBu} + 2\text{H}]^+$, $\text{C}_{38}\text{H}_{42}\text{N}_{11}\text{O}_{11}^+$; calc. 828.3054). Anal. calc. for $\text{C}_{42}\text{H}_{49}\text{N}_{11}\text{O}_{11} \cdot \text{CH}_4\text{O}$ (915.96): C 56.39, H 5.83, N 16.82; found: C 56.30, H 5.76, N 17.01.

tert-Butyl 8- $\{[1-(2\text{-Ethoxy-2-oxoethyl})hydrazino\}methyl\}$ adenine-9-acetyl-(9 \rightarrow 6 \rightarrow 3-N)-6- $\{[1-(2\text{-ethoxy-2-oxoethyl})hydrazino\}methyl\}uracil-1\text{-acetate}$ (= Ethyl $\{1-[6\text{-Amino-9-}[2-[(3- $\{2\text{-tert-bu-}$$

toxy)-2-oxoethyl]-2,6-dioxo-1,2,3,6-tetrahydropyrimidin-4-yl)methyl]-2-(2-ethoxy-2-oxoethyl)hydrazinyl]-2-oxoethyl]-9H-purin-8-yl)methyl]hydrazinyl]acetate; **13**). A soln. of **12** (290 mg, 0.33 mmol) in DMF (10 ml) was treated dropwise with piperidine (0.32 ml, 3.3 mmol), stirred for 30 min at r.t., and evaporated. The solid residue was suspended in Et₂O (10 ml) and washed with Et₂O (5 × 10 ml). Filtration gave **13** (215 mg, 99%). White powder. *R_f* (CH₂Cl₂/MeOH 9:1) 0.28. M.p. > 185° (dec.). UV (MeOH): 264 (24800). IR (ATR): 3408_w, 3318_w, 3198_w (br.), 2982_w, 2773_w (br.), 1733_m, 1703_s, 1678_s, 1647_s, 1610_m, 1534_w, 1456_m, 1441_m, 1421_m, 1394_m, 1372_m, 1322_w, 1292_w, 1273_w, 1235_m, 1196_s, 1154_s, 1113_m, 1075_w, 1024_m, 1002_w, 983_w, 960_m, 932_w, 890_w, 844_m, 818_m. ¹H-NMR (300 MHz, (D₆)DMSO; *ca.* 3:2 mixture of rotamers; assignments based on a HSQC and a HMBC spectrum): 11.40 (br. s, H-N(3/I)); 9.65 (0.6 H), 8.96 (0.4 H) (2s, HN-NCH₂C(6/I)); 8.05 (0.6 H), 7.99 (0.4 H) (2s, H-C(2/II)); 7.17 (1.2 H), 7.10 (0.8 H) (2 br. s, H₂N-C(6/II)); 5.62 (0.6 H), 5.59 (0.4 H) (2s, H-C(5/I)); 5.39 (br. d, *J* = 17.7, 0.2 CH₂-N(9/II)); 4.91–4.87 (br. m, 0.8 CH₂-N(9/II)); 5.07 (0.4 H), 4.65 (0.4 H) (2 br. d, *J* = 17.4, 0.4 CH₂-N(1/I)); 4.86 (s, 0.6 CH₂-N(1/I)); 4.22–4.07 (*m*, 2 MeCH₂O); 4.04 (1.2 H), 3.99 (0.8 H) (2 br. s, CH₂-C(8/II)); 3.92 (0.9 H), 3.78 (1.1 H) (2s, CH₂NCH₂C(6/I)); 3.86 (0.6 H), 3.64 (0.6 H) (2 br. d, *J* = 14.0, 0.6 CH₂-C(6/I)); 3.80 (s, 0.4 CH₂-C(6/I)); 3.73 (br. s, H₂N-N); 3.50 (0.6 H), 3.48 (1.4 H) (2s, CH₂NCH₂C(8/II)); 1.43 (3.8 H), 1.35 (5.2 H) (2s, *t*-Bu); 1.27–1.17 (*m*, 2 MeCH₂O). ¹³C-NMR (100 MHz, (D₆)DMSO; *ca.* 3:2 mixture of rotamers; assignments based on a HSQC and a HMBC spectrum): signals of the major rotamer: 167.98 (s, CO₂Bu); 165.92 (s, C(O)CH₂N(9/II)); 162.49 (s, C(4/I)); 155.34 (s, C(6/II)); 151.65 (s, C(2/I)); 151.20 (s, C(4/II)); 150.62 (s, C(6/I)); 148.28 (s, C(8/II)); 117.39 (s, C(5/II)); 103.86 (d, C(5/I)); 81.50 (s, Me₃C); 56.20 (*t*, CH₂-C(6/I)); 56.60 (*t*, CH₂-C(8/II)); 45.19 (*t*, CH₂-N(1/I)); 43.24 (*t*, CH₂-N(9/II)); 27.54 (*q*, Me₃C); signals of the minor rotamer: 169.35 (s, C(O)CH₂N(9/II)); 167.66 (s, CO₂Bu); 162.59 (s, C(4/I)); 155.23 (s, C(6/II)); 151.82 (s, C(2/I)); 151.14 (s, C(4/II)); 149.57 (s, C(6/I)); 148.68 (s, C(8/II)); 117.33 (s, C(5/II)); 105.39 (d, C(5/I)); 81.77 (s, Me₃C); 57.64 (*t*, CH₂-C(6/I)); 56.45 (*t*, CH₂-C(8/II)); 45.34 (*t*, CH₂-N(1/I)); 42.67 (*t*, CH₂-N(9/II)); 27.63 (*q*, Me₃C); signals of both rotamers: 170.20, 170.04, 169.24, 169.23 (4s, 2 CO₂Et); 152.27 (d, C(2/II)); 60.66, 60.38, 59.87, 59.84 (4t, 2 MeCH₂O); 59.66 (*t*, CH₂NCH₂C(8/II)); 59.22 (*t*, CH₂NCH₂C(6/I)); 14.06, 14.02, 13.98, 13.95 (4q, 2 MeCH₂O). HR-MALDI-MS: 684.2849 (19, [M + Na]⁺, C₂₇H₃₉N₁₁NaO₉⁺; calc. 684.2824), 662.3000 (100, [M + H]⁺, C₂₇H₄₀N₁₁O₉⁺; calc. 662.3005), 606.2385 (41, [M - Bu + 2 H]⁺, C₂₃H₃₂N₁₁O₉⁺; calc. 606.2379).

8-[(1-(2-Ethoxy-2-oxoethyl)-2-[[9H-fluoren-9-yl)methoxy]carbonyl]hydrazino)methyl]-N⁶-(benzyloxy)carbonyl]adenine-9-acetyl-(9² → 8³-N)-8-[[1-(2-ethoxy-2-oxoethyl)hydrazino)methyl]-N⁶-[(benzyloxy)carbonyl]adenine-9-acetic Acid (= (6-[[[(benzyloxy)carbonyl]amino]-8-[[2-[[6-[[[(benzyloxy)carbonyl]amino]-8-[[1-(2-ethoxy-2-oxoethyl)-2-[[9H-fluoren-9-yl)methoxy]carbonyl]hydrazinyl]methyl]-9H-purin-9-yl]acetyl]-1-(2-ethoxy-2-oxoethyl)hydrazinyl]methyl]-9H-purin-9-yl]acetic Acid; **16**). A soln. of **15**¹³ (1.32 g, 1.12 mmol) in CH₂Cl₂ (20 ml) was treated with Et₃SiH (1.8 ml, 11.2 mmol) and TFA (2.5 ml, 34 mmol), stirred for 2 d at r.t., and evaporated. The solid residue was washed with Et₂O (5 × 20 ml). MPLC (CH₂Cl₂/MeOH 85:15 → 80:20, flow: 30 ml/min) gave **16** (863 mg, 69%). Yellow foam. *R_f* (CH₂Cl₂/MeOH 8:2) 0.57. UV (CHCl₃): 270 (54200), 301 (5300). IR (ATR): 3674–2351_w (br.), 3230_w (br.), 2981_w, 1727_s (br.), 1612_m, 1592_m, 1533_w, 1497_m, 1450_m, 1391_m, 1320_m, 1296_m, 1199_s, 1163_s, 1101_m, 1028_m, 969_w, 897_w, 855_w. ¹H-NMR (400 MHz, (D₆)DMSO; *ca.* 1:1 mixture of rotamers; assignments based on a HSQC and a HMBC spectrum): 14.22–12.45 (br. s, CO₂H); 10.67 (0.6 H), 10.61 (0.5 H), 10.55 (0.5 H), 10.48 (0.4) (4s, 2 HN-C(6)); 9.81 (0.5 H), 9.13 (0.5 H) (2s, HN-NCH₂C(8/I)); 8.79 (0.5 H), 8.75 (0.5 H) (2s, HN-NCH₂C(8/II)); 8.63 (0.5 H), 8.56 (0.5 H), 8.39 (0.5 H), 8.08 (0.5 H) (4s, 2 H-C(2)); 7.84–7.18 (*m*, 18 arom. H); 5.86 (0.5 H) (br. d, *J* = 17.2, CH₂-N(9)); 5.46–5.35 (1.5 H) (*m*, CH₂-N(9)); 5.23 (2.1 H) (s, CH₂-N(9), PhCH₂); 5.18–5.16 (3.9 H) (*m*, CH₂-N(9), PhCH₂); 4.54 (0.2 H); 4.50 (0.3 H); 4.42 (1.5 H) (s, CH₂-C(8)); 4.23–4.00 (9.5 H) (*m*, CH₂-C(8), 2 MeCH₂O, CH₂-C(9), H-C(9)); 3.78 (1.0 H), 3.68 (2.0 H) (2s, 2 CH₂NCH₂C(8)); 3.61 (s, 0.2 H); 3.58 (s, 0.3 H); 1.19–1.12 (*m*, 2 MeCH₂O). ¹³C-NMR (100 MHz, (D₆)DMSO; *ca.* 1:1 mixture of rotamers; assignments based on a HSQC and a HMBC spectrum): 169.40, 169.22, 169.17, 169.11, 169.00, 168.91, 165.66 (7s, CO₂H, 2 CO₂Et, C(O)CH₂N(9/II)); 155.07 (br. s, N-NCO₂); 153.39, 153.29 (2s, 2 C(4)); 152.00, 151.93 (2s, 2 C(6)-NCO₂); 151.59–151.52, 151.29–151.13 (2 br. s, 2 C(8)); 151.00, 150.89, 150.37, 150.21 (4d,

¹³) Dimer **15** was synthesized analogously to dimers **5** and **9**, without purification and analysis.

5.09 (br. s, 0.9 H), 5.06 (br. s, 1.1 H), 4.99 (br. s, 0.5 H), 4.92 (br. s, 0.9 H), 4.91 (br. s, 1.6 H), 4.71 (br. s, 1.4 H), 4.55–4.43 (br. m, 0.4 H) (CH₂–N(1/I,II), CH₂–N(9/III,IV)); 4.27–3.84 (br. m, CH₂–C(9'), H–C(9')), 4 MeCH₂O, CH₂–C(8/III,IV)); 3.79 (1.0 H), 3.75 (4.0 H), 3.71 (3.0 H), 3.68–3.58 (br. m, 4.0 H) (CH₂–C(6/I,II), CH₂NCH₂C(6/I,II), CH₂NCH₂C(8/III,IV)); 1.41 (2.0 H), 1.38 (7.0 H) (2s, *t*-Bu); 1.25–1.10 (m, 4 MeCH₂O). ¹³C-NMR (75 MHz, (D₆)DMSO; mixture of rotamers): 169.40, 169.36, 169.32, 169.23, 169.20, 169.14, 169.11, 169.04, 168.01 (9s, 4 CO₂Et, CO₂^tBu, C(O)CH₂N(1/I,II), C(O)CH₂N(9/III,IV)); 162.64, 162.42, 162.39 (3s, C(4/I,II)); 155.46, 155.38, 155.33, 155.26 (4s, N–NCO₂); 152.43, 152.33, 152.22, 152.14, 151.74, 151.61, 151.55, 151.14, 151.08, 150.94 (9s, 1d, C(2/I,II), C(6/I,II), C(2/III,IV), C(4/III,IV), C(6/III,IV), C(8/III,IV)); 143.53 (br. s); 140.58 (br. s); 127.54 (br. d); 126.95 (br. d); 125.03 (br. d); 119.98 (br. d); 117.34, 117.32 (2s, C(5/III,IV)); 103.74 (br. d, C(5/I,II)); 81.46 (s, Me₃C); 65.63 (t, CH₂–C(9')); 60.44, 60.31, 60.19 (3t, 4 MeCH₂O); 56.63–56.31 (br. t, CH₂–C(6/I,II), CH₂NCH₂C(6/I,II), CH₂–C(8/III,IV), CH₂NCH₂C(8/III,IV)); 48.53 (d, C(9')); 46.51–46.45 (br. t, CH₂–N(1/I,II)); 45.16 (t, CH₂–N(9/III,IV)); 27.55 (q, Me₃C); 13.87 (br. q, 4 MeCH₂O). HR-MALDI-MS: 1494.5791 (59), 1493.5733 (100, [M + Na]⁺, C₆₅H₇₉N₂₂NaO₁₉); calc. 1493.5706), 1472.6047 (17), 1471.5986 (39, [M + H]⁺, C₆₅H₇₉N₂₂O₁₉); calc. 1471.5886).

8-*[1-(2-Ethoxy-2-oxoethyl)-2-acetylhydrazino]methyl]adenine-9-acetyl-[9² → 6³-N]-6-*[1-(2-ethoxy-2-oxoethyl)hydrazino]methyl]uracil-1-acetyl-[1² → 8³-N]-8-*[1-(2-ethoxy-2-oxoethyl)hydrazino]methyl]adenine-9-acetyl]₃-[9² → 6³-N]-6-*[1-(2-ethoxy-2-oxoethyl)hydrazino]methyl]uracil-1-acetamide* (= *Ethyl [2-Acetyl-1-[6-amino-9-[2-[2-[3-(2-[2-[3-(2-[2-[3-(2-[2-[6-amino-9-[2-[2-[3-(2-[2-[6-amino-9-[2-[2-[3-(2-amino-2-oxoethyl)-2,6-dioxo-1,2,3,6-tetrahydropyrimidin-4-yl]methyl]-2-(2-ethoxy-2-oxoethyl)hydrazinyl]-2-oxoethyl]-9H-purin-8-yl)methyl]-2-(2-ethoxy-2-oxoethyl)hydrazinyl]-2-oxoethyl]-2,6-dioxo-1,2,3,6-tetrahydropyrimidin-4-yl]methyl]-2-(2-ethoxy-2-oxoethyl)hydrazinyl]-2-oxoethyl]-9H-purin-8-yl)methyl]-2-(2-ethoxy-2-oxoethyl)hydrazinyl]-2-oxoethyl]-2,6-dioxo-1,2,3,6-tetrahydropyrimidin-4-yl]methyl]-2-(2-ethoxy-2-oxoethyl)hydrazinyl]-2-oxoethyl]-9H-purin-8-yl)methyl]hydrazinyl]acetate*; **24**). a) *Solid-Phase Synthesis*. 1. *Swelling of the Rink Amide MBHA Resin*. The resin (34.7 mg, 0.025 mmol of reactive sites, loading: 0.72 mmol/g) was treated with CH₂Cl₂ (5 ml) for 1 h.***

2. *Fmoc Deprotection of the Rink Amide MBHA Resin*. The resin was treated with a soln. of 20% piperidine in DMSO (0.5 ml) for 10 min, washed with DMSO (5 × 1 ml), treated with a soln. of 20% piperidine in DMSO (0.5 ml) for 10 min, and washed with DMSO (10 × 0.5 ml).

3. *Coupling of the 1st Monomer (Double Coupling)*. The resin was treated with a soln. of **4** (32.7 mg, 0.063 mmol) and HATU (22.8 mg, 0.06 mmol) in DMSO (0.3 ml) and EtNⁱPr₂ (22 μl, 0.13 mmol) for 4 h. After washing with DMSO (10 × 0.5 ml), the resin was treated with a soln. of **4** (32.7 mg, 0.063 mmol) and HATU (22.8 mg, 0.06 mmol) in DMSO (0.3 ml), and EtNⁱPr₂ (22 μl, 0.13 mmol) for 4 h, and washed with DMSO (10 × 0.5 ml) and CH₂Cl₂ (5 × 1 ml).

4. *Acetylation (Capping) of the Unreacted Sites of the Rink Amide MBHA Resin*. The resin was treated with a 0.5M soln. of Ac₂O and EtNⁱPr₂ in NMP (0.75 ml) for 15 min, washed with DMSO (5 × 1 ml), treated with a 0.5M soln. of Ac₂O and EtNⁱPr₂ in NMP (0.75 ml) for 15 min, and washed with DMSO (10 × 0.5 ml) and CH₂Cl₂ (5 × 1 ml).

5. *Fmoc Deprotection of the Growing Oligomer*. The resin was treated with CH₂Cl₂ (5 ml) for 1 h (swelling), then with a soln. of 2% DBU in DMSO (2 ml) for 3 min, washed with DMSO (5 × 1 ml), treated with a soln. of 2% DBU in DMSO (2 ml) for 3 min (3 ×), and washed with DMSO (10 × 0.5 ml).

6. *Coupling of the 2nd Monomer*. The resin was treated with a soln. of **8** (42.5 mg, 0.063 mmol) and HATU (22.8 mg, 0.06 mmol) in DMSO (0.4 ml), and EtNⁱPr₂ (22 μl, 0.13 mmol) for 4 h, and washed with DMSO (10 × 0.5 ml) and CH₂Cl₂ (5 × 1 ml).

7. *Fmoc Deprotection of the Growing Oligomer*. As described under 5.

8. *Coupling of the 3rd Monomer*. The resin was treated with a soln. of **4** (32.7 mg, 0.063 mmol) and HATU (22.8 mg, 0.06 mmol) in DMSO (0.3 ml), and EtNⁱPr₂ (22 μl, 0.13 mmol) for 4 h, and washed with DMSO (10 × 0.5 ml) and CH₂Cl₂ (5 × 1 ml).

9. *Fmoc Deprotection of the Growing Oligomer*. As described under 5.

10. *Coupling of the 4th Monomer*. As described under 6.

11. *Fmoc Deprotection of the Growing Oligomer*. As described under 5.

12. *Coupling of the 5th Monomer.* As described under 8.
13. *Fmoc Deprotection of the Growing Oligomer.* As described under 5.
14. *Coupling of the 6th Monomer.* As described under 6.
15. *Fmoc Deprotection of the Growing Oligomer.* As described under 5.
16. *Coupling of the 7th Monomer.* As described under 8.
17. *Fmoc Deprotection of the Growing Oligomer.* As described under 5.
18. *Coupling of the 8th Monomer.* As described under 6.
19. *Fmoc Deprotection of the Octamer.* As described under 5.

20. *N-Terminal Acetylation of the Octamer.* The resin was treated with a 0.5M soln. of Ac₂O and EtNⁱPr₂ in NMP (0.75 ml) for 15 min, washed with NMP (5 × 1 ml), treated with a 0.5M soln. of Ac₂O and EtNⁱPr₂ in NMP (0.75 ml) for 15 min, and washed with NMP (10 × 0.5 ml) and CH₂Cl₂ (5 × 1 ml).

21. *Cleavage of the Octamer from the Resin.* A suspension of the resin in TFA/ⁱPr₃SiH 97:3 (2 ml) was stirred for 1.5 h at r.t. and then dried. The solid residue and the resin were suspended in MeCN (5 ml), neutralized with Amberlite® IRA-68 to pH 7, and filtered (washing with 20 × 1 ml of MeCN). The combined filtrate and washings were evaporated, affording the crude Cbz-protected octamer (67 mg).

b) *Cbz Deprotection.* A suspension of Pd(OAc)₂ (240 mg, 1.07 mmol) in MeOH (3 ml) was stirred under H₂ for 1.5 h at r.t., treated with a soln. of the crude Cbz-protected octamer (67 mg, obtained from the solid-phase synthesis) in MeOH (2 ml), stirred for 22 h, and filtered through Celite (washing with 30 ml of MeOH). Evaporation of the filtrate and HPLC (*LiChrosphere 100 NH₂*, 5 μm, 250 × 25 mm, MeCN/H₂O 95:5 → 80:20, flow: 10 ml/min) gave **24** (3 mg, 5%). White powder. UV (H₂O): 265 (34400). ¹H-NMR (500 MHz, H₂O/D₂O 9:1; excitation sculpting, 5.7°; mixture of rotamers): 9.82, 9.77, 9.65 (3 br. s, H–N(3/I,III,V,VII)); 7.94, 7.90, 7.88, 7.80 (4s, H–C(2/II,IV,VI,VIII)); 7.02, 6.60 (2 br. s, HN–NCH₂C(6/I,III,V,VII), HN–NCH₂C(8/II,IV,VI,VIII)); 5.81–5.47, 5.40 (4 br. s, H–C(5/I,III,V,VII)); 4.01–3.92 (*m*, 8 MeCH₂O); 3.66, 3.60, 3.57, 3.51, 3.45, 3.37, 3.33 (7 br. s, CH₂–C(6/I,III,V,VII), CH₂–C(8/II,IV,VI,VIII), CH₂NCH₂C(6/I,III,V,VII), CH₂NCH₂C(8/II,IV,VI,VIII)); 1.03–0.98 (*m*, 8 MeCH₂O). HR-MALDI-MS: 2430.9003 (66, [M + Na]⁺, C₉₄H₁₂₁N₄₅NaO₃₃; calc. 2430.9066), 2431.8970 (100), 2432.8995 (73), 2433.9076 (34), 2434.9168 (12). HPLC/MS (*Waters Atlantis dC18-3*, 100 × 3 mm, MeCN/H₂O/HCO₂H 20:80:0.1 → 95:5:0.1; flow: 0.2 ml/min; *Finnigan LCQ Deca Ion Trap* ESI-MS): *t*_R 15.7 min (1205 (24, [M + 2 H]²⁺), 804 (100, [M + 3 H]³⁺), 604 (52, [M + 4 H]⁴⁺)).

8-[[1-(2-Ethoxy-2-oxoethyl)-2-acetylhydrazino]methyl]adenine-9-acetyl-[(9² → 8³-N)-8-[[1-(2-ethoxy-2-oxoethyl)hydrazino]methyl]adenine-9-acetyl]₅-(9² → 6³-N)-6-[[1-(2-ethoxy-2-oxoethyl)hydrazino]methyl]uracil-1-acetyl-[(1² → 6³-N)-6-[[1-(2-ethoxy-2-oxoethyl)hydrazino]methyl]uracil-1-acetyl]₂-(1² → 6³-N)-6-[[1-(2-ethoxy-2-oxoethyl)hydrazino]methyl]uracil-1-acetamide (= Ethyl [2-Acetyl-1-[(6-amino-9-[2-[2-[[6-amino-9-(2-[2-[[6-amino-9-(2-[2-[[3-[2-[2-[[3-[2-[2-[[3-[2-[2-[[3-(2-amino-2-oxoethyl)-2,6-dioxo-1,2,3,6-tetrahydropyrimidin-4-yl]methyl]-2-(2-ethoxy-2-oxoethyl)hydrazinyl]-2-oxoethyl)-2,6-dioxo-1,2,3,6-tetrahydropyrimidin-4-yl]methyl]-2-(2-ethoxy-2-oxoethyl)hydrazinyl]-2-oxoethyl)-2,6-dioxo-1,2,3,6-tetrahydropyrimidin-4-yl]methyl]-2-(2-ethoxy-2-oxoethyl)hydrazinyl]-2-oxoethyl)-2,6-dioxo-1,2,3,6-tetrahydropyrimidin-4-yl]methyl]-2-(2-ethoxy-2-oxoethyl)hydrazinyl]-2-oxoethyl)-9H-purin-8-yl]methyl]-2-(2-ethoxy-2-oxoethyl)hydrazinyl]-2-oxoethyl]-9H-purin-8-yl]methyl]-2-(2-ethoxy-2-oxoethyl)hydrazinyl]-2-oxoethyl]-9H-purin-8-yl]methyl]hydraziny]acetate; **26**). a) *Solid-Phase Synthesis.* 1. *Swelling of the Rink Amide MBHA Resin.* The resin (69.4 mg, 0.05 mmol of reactive sites; loading: 0.72 mmol/g) was treated with CH₂Cl₂ (5 ml) for 1 h.

2. *Fmoc Deprotection of the Rink Amide MBHA Resin.* The resin was treated with a soln. of 20% piperidine in DMSO (1 ml) for 10 min, washed with DMSO (5 × 1 ml), treated with a soln. of 20% piperidine in DMSO (1 ml) for 10 min, and washed with DMSO (10 × 2 ml).

3. *Coupling of the 1st Monomer.* The resin was treated with a soln. of **4** (65.3 mg, 0.13 mmol) and HATU (46.6 mg, 0.12 mmol) in DMSO (0.3 ml), and EtNⁱPr₂ (44 μl, 0.25 mmol) for 6 h, and washed with DMSO (10 × 2 ml).

4. *Acetylation (Capping) of the Unreacted Sites of the Rink Amide MBHA Resin.* The resin was treated with a 0.5M soln. of Ac₂O and EtNⁱPr₂ in NMP (1.5 ml) for 15 min, washed with NMP (10 × 2 ml),

treated with a 0.5M soln. of Ac_2O and $\text{Et}_3\text{N}^i\text{Pr}_2$ in DMSO (1.5 ml) for 15 min, and washed with DMSO (10×2 ml).

5. *Fmoc Deprotection of the Growing Oligomer.* The resin was treated with a soln. of 4% DBU in DMSO (2 ml) for 2 min, washed with DMSO (5×1 ml), treated with a soln. of 4% DBU in DMSO (2 ml) for 2 min ($3 \times$), and washed with DMSO (10×2 ml).

6. *Coupling of the 2nd Monomer.* As described under 3, but coupling for 4 h.

7. *Fmoc Deprotection of the Growing Oligomer.* As described under 5.

8. *Coupling of the 3rd Monomer.* As described under 6.

9. *Fmoc Deprotection of the Growing Oligomer.* As described under 5.

10. *Coupling of the 4rd Monomer.* As described under 6.

11. *Fmoc Deprotection of the Growing Oligomer.* As described under 5.

12. *Coupling of the 5th Monomer.* The resin was treated with a soln. of **8** (85.0 mg, 0.13 mmol) and HATU (46.6 mg, 0.12 mmol) in DMSO (0.3 ml), and $\text{Et}_3\text{N}^i\text{Pr}_2$ (44 μl , 0.25 mmol) for 4 h, and washed with DMSO (10×2 ml).

13. *Fmoc Deprotection of the Growing Oligomer.* As described under 5.

14. *Coupling of the 6th Monomer.* As described under 12.

15. *Fmoc Deprotection of the Growing Oligomer.* As described under 5.

16. *Coupling of the 7th Monomer.* As described under 12.

17. *Fmoc Deprotection of the Growing Oligomer.* As described under 5.

18. *Coupling of the 8th Monomer.* As described under 12.

19. *Fmoc Deprotection of the Octamer.* As described under 5.

20. *N-Terminal Acetylation of the Octamer.* As described under 4. The resin was washed with CH_2Cl_2 and EtOH, and dried *in vacuo*.

21. *Cleavage of the Octamer from the Resin.* A suspension of the resin in TFA/ $^i\text{Pr}_3\text{SiH}$ 97:3 (1.5 ml) was stirred for 3 h at r.t. The resin was filtered off and washed with TFA/ $^i\text{Pr}_3\text{SiH}$ 97:3 (1 ml).

b) *Cbz Deprotection.* The filtrate resulting from the cleavage of the octamer from the resin in TFA/ $^i\text{Pr}_3\text{SiH}$ 97:3 (2.5 ml; see 21) was heated to 80° and stirred for 5 h. The volume of TFA was reduced in a stream of N_2 , and the residue was treated with Et_2O . The precipitate was filtered off and washed with Et_2O . A soln. of the solid in MeCN/ H_2O 1:1 (0.5 ml) was passed through a column of Amberlite® IRA-68 to obtain a soln. with pH 7. Evaporation and HPLC (*LiChrosphere 100 NH₂*, 5 μm , 250×25 mm, MeCN/ H_2O 8:2 \rightarrow 1:1; flow: 10 ml/min) gave **26** (6.0 mg, 5%). White powder. HPLC/MS (*Waters Atlantis dC18-3*, 100×3 mm; MeCN/ $\text{H}_2\text{O}/\text{HCO}_2\text{H}$ 10:90:0.1 \rightarrow 95:5:0.1; flow: 0.2 ml/min, *Finnigan LCQ Deca Ion Trap* ESI-MS): t_{R} 24.2 min (1205 (100, $[M+2\text{H}]^{2+}$), 804 (34, $[M+3\text{H}]^{3+}$)).

8-[[1-(2-Ethoxy-2-oxoethyl)-2-acetylhydrazino]methyl]adenine-9-acetyl-($9^2 \rightarrow 8^3\text{-N}$)-8-[[1-(2-ethoxy-2-oxoethyl)hydrazino]methyl]adenine-9-acetyl-($9^2 \rightarrow 6^3\text{-N}$)-6-[[1-(2-ethoxy-2-oxoethyl)hydrazino]methyl]uracil-1-acetyl-($1^2 \rightarrow 6^3\text{-N}$)-6-[[1-(2-ethoxy-2-oxoethyl)hydrazino]methyl]uracil-1-acetyl-($1^2 \rightarrow 8^3\text{-N}$)-8-[[1-(2-ethoxy-2-oxoethyl)hydrazino]methyl]adenine-9-acetyl-($9^2 \rightarrow 8^3\text{-N}$)-8-[[1-(2-ethoxy-2-oxoethyl)hydrazino]methyl]adenine-9-acetyl-($9^2 \rightarrow 6^3\text{-N}$)-6-[[1-(2-ethoxy-2-oxoethyl)hydrazino]methyl]uracil-1-acetyl-($1^2 \rightarrow 6^3\text{-N}$)-6-[[1-(2-ethoxy-2-oxoethyl)hydrazino]methyl]uracil-1-acetamide (= Ethyl [2-Acetyl-1-[(6-amino-9-[2-[2-[[6-amino-9-(2-[2-[(3-[2-[2-[[3-(2-[2-[(6-amino-9-[2-[2-[[6-amino-9-(2-[2-[(3-[2-[2-[[3-(2-[2-[[3-(2-amino-2-oxoethyl)-2,6-dioxo-1,2,3,6-tetrahydropyrimidin-4-yl]methyl)-2-(2-ethoxy-2-oxoethyl)hydrazinyl]-2-oxoethyl)-2,6-dioxo-1,2,3,6-tetrahydropyrimidin-4-yl]methyl)-2-(2-ethoxy-2-oxoethyl)hydrazinyl]-2-oxoethyl)-9H-purin-8-yl]methyl)-2-(2-ethoxy-2-oxoethyl)hydrazinyl]-2-oxoethyl)-9H-purin-8-yl]methyl)-2-(2-ethoxy-2-oxoethyl)hydrazinyl]-2-oxoethyl)-2,6-dioxo-1,2,3,6-tetrahydropyrimidin-4-yl]methyl)-2-(2-ethoxy-2-oxoethyl)hydrazinyl]-2-oxoethyl)-9H-purin-8-yl]methyl]-2-(2-ethoxy-2-oxoethyl)hydrazinyl]-2-oxoethyl)-9H-purin-8-yl]methyl]hydrazinyl]acetate; **28**). a) *Solid-Phase Synthesis.* 1. *Swelling of the Rink Amide MBHA Resin.* The resin (34.7 mg, 0.025 mmol of reactive sites; loading: 0.72 mmol/g) was treated with CH_2Cl_2 (5 ml) for 1 h.

2. *Fmoc Deprotection of the Rink Amide MBHA Resin.* The resin was treated with a soln. of 20% piperidine in DMSO (0.5 ml) for 10 min, washed with DMSO (5×1 ml), treated with a soln. of 20% piperidine in DMSO (0.5 ml) for 10 min, and washed with DMSO (10×0.5 ml).

3. *Coupling of the 1st Monomer.* The resin was treated with a soln. of **4** (32.7 mg, 0.063 mmol) and HATU (22.8 mg, 0.06 mmol) in DMSO (0.3 ml), and EtNⁱPr₂ (22 μl, 0.13 mmol) for 4 h, and washed with DMSO (10 × 0.5 ml) and CH₂Cl₂ (5 × 1 ml).

4. *Acetylation (Capping) of the Unreacted Sites of the Rink Amide MBHA Resin.* The resin was treated with a 0.5M soln. of Ac₂O and EtNⁱPr₂ in DMSO (0.75 ml) for 15 min, washed with DMSO (5 × 1 ml), treated with a 0.5M soln. of Ac₂O and EtNⁱPr₂ in DMSO (0.75 ml) for 15 min, and washed with DMSO (10 × 0.5 ml) and CH₂Cl₂ (5 × 1 ml).

5. *Fmoc Deprotection of the Growing Oligomer.* The resin was treated with CH₂Cl₂ (5 ml) for 1 h (swelling), then with a soln. of 2% DBU in DMSO (2 ml) for 3 min, washed with DMSO (5 × 1 ml), treated with a soln. of 2% DBU in DMSO (2 ml) for 3 min (3 ×), and washed with DMSO (10 × 0.5 ml).

6. *Coupling of the 2nd Monomer.* As described under 3.

7. *Fmoc Deprotection of the Growing Oligomer.* As described under 5.

8. *Coupling of the 3rd Monomer.* The resin was treated with a soln. of **8** (42.5 mg, 0.063 mmol) and HATU (22.8 mg, 0.06 mmol) in DMSO (0.3 ml), and EtNⁱPr₂ (22 μl, 0.13 mmol) for 4 h, and washed with DMSO (10 × 0.5 ml) and CH₂Cl₂ (5 × 1 ml).

9. *Fmoc Deprotection of the Growing Oligomer.* As described under 5.

10. *Coupling of the 4th Monomer.* As described under 8.

11. *Fmoc Deprotection of the Growing Oligomer.* As described under 5.

12. *Coupling of the 5th Monomer.* As described under 3.

13. *Fmoc Deprotection of the Growing Oligomer.* As described under 5.

14. *Coupling of the 6th Monomer.* As described under 3.

15. *Fmoc Deprotection of the Growing Oligomer.* As described under 5.

16. *Coupling of the 7th Monomer.* The resin was treated with a soln. of **8** (42.5 mg, 0.063 mmol) and HATU (22.8 mg, 0.06 mmol) in DMSO (0.4 ml), and EtNⁱPr₂ (22 μl, 0.13 mmol) for 4 h, and washed with DMSO (10 × 0.5 ml) and CH₂Cl₂ (5 × 1 ml).

17. *Fmoc Deprotection of the Growing Oligomer.* As described under 5.

18. *Coupling of the 8th Monomer.* The resin was treated with a soln. of **8** (42.5 mg, 0.063 mmol) and HATU (22.8 mg, 0.06 mmol) in DMSO (0.5 ml), and EtNⁱPr₂ (22 μl, 0.13 mmol) for 4 h, and washed with DMSO (10 × 0.5 ml) and CH₂Cl₂ (5 × 1 ml).

19. *Fmoc Deprotection of the Octamer.* As described under 5.

20. *N-Terminal Acetylation of the Octamer.* As described under 4.

21. *Cleavage of the Octamer from the Resin.* A suspension of the resin in TFA/ⁱPr₃SiH 97:3 (2 ml) was stirred for 1.5 h at r.t., and evaporated. The solid residue and the resin were suspended in MeOH (5 ml), and filtered (washing with 20 × 1 ml of MeOH). The combined filtrate and washings were evaporated to afford the crude Cbz-protected octamer (48 mg).

b) *Cbz Deprotection.* A soln. of the crude Cbz-protected octamer (48 mg, obtained from the solid-phase synthesis) in TFA/ⁱPr₃SiH 97:3 (2 ml) was heated to 80°, stirred for 5 h, and evaporated. A soln. of the residue in MeCN/H₂O 1:1 (5 ml) was neutralized with Amberlite® IRA-68 to pH 7. Filtration, evaporation, and HPLC (*LiChrosphere 100 NH₂*, 5 μm, 250 × 25 mm; MeCN/H₂O 8:2 → 1:1; flow: 10 ml/min) gave **28** (5 mg, 8%). White powder. UV (H₂O): 263 (37000). ¹H-NMR (500 MHz, H₂O/D₂O 9:1), excitation sculpting, 5.7°; mixture of rotamers): 9.71, 9.12 (2 br. s, H–N(3/I,II,V,VI)); 7.87, 7.86, 7.81, 7.76 (4s, H–C(2/III,IV,VII,VIII)); 7.04, 6.63, 6.56 (3 br. s, HN–NCH₂C(6/I,II,V,VI), HN–NCH₂C(8/III,IV,VII,VIII)); 5.69, 5.67, 5.64, 5.63, 5.57, 5.55 (6 br. s, H–C(5/I,II,V,VI)); 5.48–4.91 (br. s, CH₂–N(1/I,II,V,VI), CH₂–N(9/III,IV,VII,VIII)); 3.94 (br. s, 8 MeCH₂O); 3.71, 3.69, 3.56, 3.51, 3.48, 3.47, 3.45, 3.40–3.26 (8 br. s, CH₂–C(6/I,II,V,VI), CH₂–C(8/III,IV,VII,VIII), CH₂NCH₂C(6/I,II,V,VI), CH₂NCH₂C(8/III,IV,VII,VIII)); 1.05–0.97 (m, 8 MeCH₂O). HR-MALDI-MS: 2408.9241 (71, [M + H]⁺, C₉₄H₁₂₂N₄₅O₃₃⁺; calc. 2408.9246), 2409.9210 (100), 2410.9227 (72), 2411.9280 (35), 2412.9345 (13), 2430.9040 (61, [M + Na]⁺, C₉₄H₁₂₁N₄₅NaO₃₃⁺; calc. 2430.9066), 2431.9025 (84), 2432.9057 (62), 2433.9109 (32), 2434.9191 (11). HPLC/MS (*Waters Atlantis dC18-3*, 100 × 3 mm; MeCN/H₂O/HCO₂H 20:80:0.1 → 95:5:0.1; flow: 0.2 ml/min; *Finnigan LCQ Deca Ion Trap* ESI-MS): t_R 19.5 min (1205 (100, [M + 2 H]²⁺), 804 (54, [M + 3 H]³⁺)).

6-[[1-(2-Ethoxy-2-oxoethyl)-2-acetylhydrazino]methyl]uracil-1-acetyl-(1² → 6³-N)-6-[[1-(2-ethoxy-2-oxoethyl)hydrazino]methyl]uracil-1-acetyl-(1² → 8³-N)-8-[[1-(2-ethoxy-2-oxoethyl)hydrazino]methyl]-

adenine-9-acetyl-(9² → 8³-N)-8-[[1-(2-ethoxy-2-oxoethyl)hydrazino]methyl]adenine-9-acetyl-(9² → 6³-N)-6-[[1-(2-ethoxy-2-oxoethyl)hydrazino]methyl]uracil-1-acetyl-(1² → 6³-N)-6-[[1-(2-ethoxy-2-oxoethyl)hydrazino]methyl]uracil-1-acetyl-(1² → 8³-N)-8-[[1-(2-ethoxy-2-oxoethyl)hydrazino]methyl]adenine-9-acetyl-(9² → 8³-N)-8-[[1-(2-ethoxy-2-oxoethyl)hydrazino]methyl]adenine-9-acetamide (= Ethyl {2-Acetyl-1-[(3-{2-[2-[(3-{2-[2-[(6-amino-9-[2-2-[[6-amino-9-(2-[2-[(3-{2-[2-[(3-{2-[2-[(6-amino-9-[2-2-[[6-amino-9-(2-amino-2-oxoethyl)-9H-purin-8-yl]methyl]-2-(2-ethoxy-2-oxoethyl)hydrazinyl]-2-oxoethyl]-9H-purin-8-yl]methyl]-2-(2-ethoxy-2-oxoethyl)hydrazinyl]-2-oxoethyl]-2,6-dioxo-1,2,3,6-tetrahydropyrimidin-4-yl]methyl]-2-(2-ethoxy-2-oxoethyl)hydrazinyl]-2-oxoethyl]-2,6-dioxo-1,2,3,6-tetrahydropyrimidin-4-yl]methyl]-2-(2-ethoxy-2-oxoethyl)hydrazinyl]-2-oxoethyl)-9H-purin-8-yl]methyl]-2-(2-ethoxy-2-oxoethyl)hydrazinyl]-2-oxoethyl)-9H-purin-8-yl]methyl]-2-(2-ethoxy-2-oxoethyl)hydrazinyl]-2-oxoethyl)-2,6-dioxo-1,2,3,6-tetrahydropyrimidin-4-yl]methyl]hydrazinyl]acetate; **30**). a) *Solid-Phase Synthesis*. 1. *Swelling of the Rink Amide MBHA Resin*. The resin (69.4 mg, 0.05 mmol of reactive sites; loading: 0.72 mmol/g) was treated with CH₂Cl₂ (5 ml) for 1 h.

2. *Fmoc Removal from the Rink Amide MBHA Resin*. The resin was treated with a soln. of 20% piperidine in DMSO (1 ml) for 10 min, washed with DMSO (5 × 1 ml), treated with a soln. of 20% piperidine in DMSO (1 ml) for 10 min, and washed with DMSO (10 × 2 ml).

3. *Coupling of the 1st Monomer*. The resin was treated with a soln. of **8** (101.0 mg, 0.15 mmol), HATU (56.1 mg, 0.15 mmol), and Et₃N (44 μl, 0.25 mmol) in DMSO (0.3 ml) for 6 h, and washed with DMSO (10 × 2 ml).

4. *Acetylation (Capping) of the Unreacted Sites of the Rink Amide MBHA Resin*. The resin was treated with a 0.5M soln. of Ac₂O and Et₃N in NMP (1.5 ml) for 15 min, washed with NMP (10 × 2 ml), treated with a 0.5M soln. of Ac₂O and Et₃N in DMSO (1.5 ml) for 15 min, and washed with DMSO (10 × 2 ml).

5. *Fmoc Removal of the Growing Oligomer*. The resin was treated with a soln. of 4% DBU in DMSO (2 ml) for 2 min, washed with DMSO (5 × 1 ml), treated with a soln. of 4% DBU in DMSO (2 ml) for 2 min (3 times), and washed with DMSO (10 × 2 ml).

6. *Coupling of the 2nd Monomer*. As described under 3, but with **8** (85.0 mg, 0.13 mmol), HATU (46.6 mg, 0.12 mmol), and Et₃N (44 μl, 0.25 mmol), 4 h.

7. *Fmoc Deprotection of the Growing Oligomer*. As described under 5.

8. *Coupling of the 3rd Monomer*. The resin was treated with a soln. of **4** (65.3 mg, 0.13 mmol) and HATU (46.6 mg, 0.12 mmol) in DMSO (0.3 ml), and Et₃N (44 μl, 0.25 mmol) for 4 h, and washed with DMSO (10 × 2 ml).

9. *Fmoc Deprotection of the Growing Oligomer*. As described under 5.

10. *Coupling of the 4th Monomer*. As described under 8.

11. *Fmoc Deprotection of the Growing Oligomer*. As described under 5.

12. *Coupling of the 5th Monomer*. As described under 6.

13. *Fmoc Deprotection of the Growing Oligomer*. As described under 5.

14. *Coupling of the 6th Monomer*. As described under 6.

15. *Fmoc Deprotection of the Growing Oligomer*. As described under 5.

16. *Coupling of the 7th Monomer*. As described under 8.

17. *Fmoc Deprotection of the Growing Oligomer*. As described under 5.

18. *Coupling of the 8th Monomer*. As described under 8.

19. *Fmoc Deprotection of the Octamer*. As described under 5.

20. *N-Terminal Acetylation of the Octamer*. As described under 4. The resin was washed with CH₂Cl₂ and EtOH, and dried *in vacuo*.

21. *Cleavage of the Octamer from the Resin*. A suspension of the resin in TFA/ⁱPr₃SiH 97:3 (1.5 ml) was stirred for 3 h at r.t. The resin was filtered off and washed with TFA (1 ml). The volume of TFA was reduced with a stream of N₂, and the residue was treated with Et₂O. The precipitate was filtered off and washed with Et₂O to afford the crude Cbz-protected octamer (52 mg).

b) *Cbz Deprotection*. A soln. of the crude Cbz-protected octamer (52 mg) in TFA/ⁱPr₃SiH 97:3 (2 ml) was heated to 80° and stirred for 5 h. The volume of TFA was reduced with a stream of N₂, and the residue was treated with Et₂O. The precipitate was filtered off and washed with Et₂O. A soln. of the solid

*ethoxy-2-oxoethyl)hydrazinyl]-2-oxoethyl)-2,6-dioxo-1,2,3,6-tetrahydropyrimidin-4-yl]methyl]-2-(2-ethoxy-2-oxoethyl)hydrazinyl]-2-oxoethyl)-2,6-dioxo-1,2,3,6-tetrahydropyrimidin-4-yl)methyl]hydrazinyl]acetate; **33**). *Solid-Phase Synthesis*. 1. *Swelling of the Rink Amide MBHA Resin*. The resin (69.4 mg, 0.05 mmol of reactive sites; loading: 0.72 mmol/g) was treated with CH₂Cl₂ (5 ml) for 1 h.*

2. *Fmoc Deprotection of the Rink Amide MBHA Resin*. The resin was treated with a soln. of 20% piperidine in DMSO (1 ml) for 10 min, washed with DMSO (5 × 1 ml), treated with a soln. of 20% piperidine in DMSO (1 ml) for 10 min, and washed with DMSO (10 × 2 ml).

3. *Coupling of the 1st Monomer*. The resin was treated with a soln. of **4** (78.4 mg, 0.15 mmol) and HATU (56.1 mg, 0.15 mmol) in DMSO (0.3 ml), and Et₃N (44 μl, 0.25 mmol) for 8–10 h, and washed with DMSO (10 × 2 ml).

4. *Acetylation (Capping) of the Unreacted Sites of the Rink Amide MBHA Resin*. The resin was treated with a 0.5M soln. of Ac₂O and Et₃N in NMP (1.5 ml) for 15 min, washed with NMP (10 × 2 ml), treated with a 0.5M soln. of Ac₂O and Et₃N in DMSO (1.5 ml) for 15 min, and washed with DMSO (10 × 2 ml).

5. *Fmoc Deprotection of the Growing Oligomer*. The resin was treated with a soln. of 4% DBU in DMSO (2 ml) for 2 min, washed with DMSO (5 × 1 ml), treated with a soln. of 4% DBU in DMSO (2 ml) for 2 min (3 ×), and washed with DMSO (10 × 2 ml).

6. *Coupling of the 2nd Monomer*. As described under 3.

7. *Fmoc Deprotection of the Growing Oligomer*. As described under 5.

8. *Coupling of the 3rd Monomer*. As described under 3.

9. *Fmoc Deprotection of the Growing Oligomer*. As described under 5.

10. *Coupling of the 4th Monomer*. As described under 3.

11. *Fmoc Deprotection of the Growing Oligomer*. As described under 5.

12. *Coupling of the 5th Monomer*. As described under 3.

13. *Fmoc Deprotection of the Growing Oligomer*. As described under 5.

14. *Coupling of the 6th Monomer*. As described under 3.

15. *Fmoc Deprotection of the Growing Oligomer*. As described under 5.

16. *Coupling of the 7th Monomer*. As described under 3.

17. *Fmoc Deprotection of the Growing Oligomer*. As described under 5.

18. *Coupling of the 8th Monomer*. As described under 3.

19. *Fmoc Deprotection of the Growing Oligomer*. As described under 5.

20. *Coupling of the 9th Monomer*. As described under 3.

21. *Fmoc Deprotection of the Growing Oligomer*. As described under 5.

22. *Coupling of the 10th Monomer*. As described under 3.

23. *Fmoc Deprotection of the Growing Oligomer*. As described under 5.

24. *N-Terminal Acetylation of the Octamer*. As described under 4. The resin was washed with CH₂Cl₂ and EtOH, and dried *in vacuo*.

25. *Cleavage of the Octamer from the Resin*. A suspension of the resin in TFA/^tPr₃SiH 97:3 (1.5 ml) was stirred for 3 h at r.t. The resin was filtered off and washed with TFA/^tPr₃SiH 97:3 (1 ml). The volume of TFA was reduced in a stream of N₂, and the residue was treated with Et₂O. The precipitate was filtered off and washed with Et₂O. A soln. of the solid in MeCN/H₂O 1:1 (0.5 ml) was passed through a column of Amberlite® IRA-68 to obtain a soln. with pH 7. Evaporation and HPLC (*LiChrosphere 100 NH₂*, 5 μm, 250 × 25 mm, MeCN/H₂O 2:8 → 8:2; flow: 10 ml/min) gave **33** (2.9 mg, 2%). White powder. HPLC/MS (*Waters Atlantis dC18-3*, 100 × 3 mm; MeCN/H₂O/HCO₂H 10:90:0.1 → 95:5:0.1; flow: 0.2 ml/min; *Finnigan LCQ Deca Ion Trap ESI-MS*): *t*_R 21.1 min (1441 (100, [M + 2 H]²⁺)).

6-[[1-(2-Ethoxy-2-oxoethyl)-2-acetylhydrazino]methyl]uracil-1-acetyl-(1² → 8³-N)-8-[[1-(2-ethoxy-2-oxoethyl)hydrazino]methyl]guanino-9-acetyl-(9² → 8³-N)-8-[[1-(2-ethoxy-2-oxoethyl)hydrazino]methyl]-N⁶-[(benzyloxy)carbonyl]adenino-9-acetamide (= Ethyl (2-Acetyl-1-[[3-(2-[2-(2-amino-9-[2-[2-[9-(2-amino-2-oxoethyl)-6-[[(benzyloxy)carbonyl]amino]-9H-purin-8-yl]methyl]-2-(2-ethoxy-2-oxoethyl)-hydrazinyl]-2-oxoethyl]-6-oxo-6,9-dihydro-1H-purin-8-yl)methyl]-2-(2-ethoxy-2-oxoethyl)hydrazinyl]-2-oxoethyl)-2,6-dioxo-1,2,3,6-tetrahydropyrimidin-4-yl]methyl]hydrazinyl]acetate; **35**). By analogy to the solid-phase synthesis of **30**, **35** was obtained by sequential coupling of **8** (42.5 mg, 62.5 μmol), **34** (35.1 mg, 62.5 μmol), and **4** (32.7 mg, 62.5 μmol) in the presence of HATU (22.8 mg, 60.0 μmol) and

EtN^iPr_2 (22 μl , 125 μmol) in DMSO (0.25 ml) on a *Rink* amide MBHA or a *Sieber* amide MBHA resin (34.7 mg, 25 μmol).

Cleavage of the Trimer from the Rink Amide MBHA Resin. A suspension of the resin in $\text{TFA}/\text{Pr}_3\text{SiH}$ 97:3 (1.5 ml) was stirred for 3 h at r.t. The resin was filtered off and washed with $\text{TFA}/\text{Pr}_3\text{SiH}$ 97:3 (1 ml). The volume of TFA was reduced in a stream of N_2 , and the residue was triturated with Et_2O . The precipitate was filtered off and washed with Et_2O to afford crude **35**.

Cleavage of the Trimer from the Sieber Amide Resin. The resin was treated for 4×15 min with a soln. of $\text{CH}_2\text{Cl}_2/\text{TFA}$ 99:1 (2 ml), and washed with $\text{CH}_2\text{Cl}_2/\text{TFA}$ 99:1 (2 ml) and EtOH (2 ml). The soln. was evaporated at r.t., and the residue was triturated with Et_2O . The solid was filtered off and washed with Et_2O to afford crude **35**. White powder. HPLC/MS (*Waters Atlantis dC18-3*, 100×3 mm; $\text{MeCN}/\text{H}_2\text{O}/\text{HCO}_2\text{H}$ 20:80:0.1 \rightarrow 95:5:0.1; flow: 0.2 ml/min; *Finnigan LCQ Deca Ion Trap* ESI-MS): t_{R} 22.9 min (1102 (100, $[\text{M} + \text{H}]^+$)).

8- $\{[1-(2\text{-Ethoxy-2-oxoethyl})-2\text{-acetylhydrazino}]methyl\}guanine-9\text{-acetyl-}(9^2 \rightarrow 6^3\text{-N})-6\text{-}\{[1-(2\text{-ethoxy-2-oxoethyl})hydrazino]methyl\}-\text{N}^6\text{-}[(benzyloxy)carbonyl]cytosine-1\text{-acetamide}$ (= Ethyl {2-Acetyl-1-[2-amino-9-[2-[2-[3-(2-amino-2-oxoethyl)-6- $\{[(benzyloxy)carbonyl]amino\}-2\text{-oxo-2,3-dihydropyrimidin-4-yl}]methyl\}-2-(2-ethoxy-2-oxoethyl)hydrazinyl]-2-oxoethyl]-6-oxo-6,9-dihydro-1H-purin-8-yl)methyl]hydrazinyl]acetate; **37**). By analogy to the solid-phase synthesis of **30**, **37** was obtained by sequential coupling of **36** (41.0 mg, 62.5 μmol) and **34** (35.1 mg, 62.5 μmol) in the presence of HATU (22.8 mg, 60.0 μmol) and EtN^iPr_2 (22 μl , 125 μmol) in DMSO (0.25 ml) on a *Sieber* amide MBHA resin (34.7 mg, 25 μmol). Cleavage of **37** from the support was performed as described for **35**. The crude product was not purified. White powder. HPLC/MS (*Waters Atlantis dC18-3*, 100×3 mm; $\text{MeCN}/\text{H}_2\text{O}/\text{HCO}_2\text{H}$ 20:80:0.1 \rightarrow 95:5:0.1; flow: 0.2 ml/min; *Finnigan LCQ Deca Ion Trap* ESI-MS): t_{R} 11.8 min (796 (100, $[\text{M} + \text{H}]^+$)).$

8- $\{[1-(2\text{-Ethoxy-2-oxoethyl})-2\text{-acetylhydrazino}]methyl\}guanine-9\text{-acetyl-}(9^2 \rightarrow 6^3\text{-N})-6\text{-}\{[1-(2\text{-ethoxy-2-oxoethyl})hydrazino]methyl\}-\text{N}^6\text{-}[(benzyloxy)carbonyl]cytosine-1\text{-acetyl-}(1^2 \rightarrow 8^3\text{-N})-8\text{-}\{[1-(2\text{-ethoxy-2-oxoethyl})hydrazino]methyl\}guanine-9\text{-acetyl-}(9^2 \rightarrow 6^3\text{-N})-6\text{-}\{[1-(2\text{-ethoxy-2-oxoethyl})hydrazino]methyl\}-\text{N}^6\text{-}[(benzyloxy)carbonyl]cytosine-1\text{-acetamide}$ (= Ethyl {2-Acetyl-1-[2-amino-9-[2-[2-[3-(2-amino-9-[2-[2-[3-(2-amino-2-oxoethyl)-6- $\{[(benzyloxy)carbonyl]amino\}-2\text{-oxo-2,3-dihydropyrimidin-4-yl}]methyl\}-2-(2-ethoxy-2-oxoethyl)hydrazinyl]-2-oxoethyl]-6-oxo-6,9-dihydro-1H-purin-8-yl)methyl]hydrazinyl]acetate; **38**). By analogy to the solid-phase synthesis of **30**, **38** was obtained by sequential coupling ($2 \times$ **36** (41.0 mg, 62.5 μmol) and $2 \times$ **34** (35.1 mg, 62.5 μmol)) in the presence of HATU (22.8 mg, 60.0 μmol) and EtN^iPr_2 (22 μl , 125 μmol) in DMSO (0.25 ml) on a *Sieber* amide MBHA resin (34.7 mg, 25 μmol). The order of the couplings can be read from the sequence (C \rightarrow N terminus). Cleavage of **38** from the support was performed as described for **35**. The crude product was not purified. Yellow powder. HPLC/MS (*Waters Atlantis dC18-3*, 100×3 mm; $\text{MeCN}/\text{H}_2\text{O}/\text{HCO}_2\text{H}$ 20:80:0.1 \rightarrow 95:5:0.1; flow: 0.2 ml/min; *Finnigan LCQ Deca Ion Trap* ESI-MS): t_{R} 20.5 min (1533 (100, $[\text{M} + \text{H}]^+$)).$

8- $\{[1-(2\text{-Ethoxy-2-oxoethyl})-2\text{-acetylhydrazino}]methyl\}guanine-9\text{-acetyl-}(9^2 \rightarrow 6^3\text{-N})-6\text{-}\{[1-(2\text{-ethoxy-2-oxoethyl})hydrazino]methyl\}-\text{N}^6\text{-}[(benzyloxy)carbonyl]cytosine-1\text{-acetyl-}(1^2 \rightarrow 8^3\text{-N})-8\text{-}\{[1-(2\text{-ethoxy-2-oxoethyl})hydrazino]methyl\}guanine-9\text{-acetyl-}(9^2 \rightarrow 6^3\text{-N})-6\text{-}\{[1-(2\text{-ethoxy-2-oxoethyl})hydrazino]methyl\}-\text{N}^6\text{-}[(benzyloxy)carbonyl]cytosine-1\text{-acetamide}$ (= Ethyl {2-Acetyl-1-[2-amino-9-[2-[2-[3-(2-amino-9-[2-[2-[3-(2-amino-2-oxoethyl)-6- $\{[(benzyloxy)carbonyl]amino\}-2\text{-oxo-2,3-dihydropyrimidin-4-yl}]methyl\}-2-(2-ethoxy-2-oxoethyl)hydrazinyl]-2-oxoethyl]-6-oxo-6,9-dihydro-1H-purin-8-yl)methyl]hydrazinyl]acetate; **39**). By analogy to the solid-phase synthesis of **30**, **39** was obtained by sequential coupling ($3 \times$ **36** (41.0 mg, 62.5 μmol) and $3 \times$ **34** (35.1 mg, 62.5 μmol)) in the presence of HATU (22.8 mg, 60.0 μmol) and EtN^iPr_2 (22 μl , 125 μmol) in DMSO (0.25 ml) on a *Sieber* amide MBHA resin (34.7 mg, 25 μmol). The order of the couplings can be read from the sequence (C \rightarrow N terminus). Cleavage of **39** from the support was performed as described$

terminus). The crude product was cleaved from the support and not purified. Yellow powder. HPLC/MS (*Waters Atlantis dC18-3*, 100 × 3 mm; MeCN/H₂O/HCO₂H 10:90:0.1 → 95:5:0.1; flow: 0.2 ml/min; *Finnigan LCQ Deca Ion Trap* ESI-MS): *t*_R 20.9 min (913 (100, [M + 3 H]³⁺)).

8-(2-Acetamidoethyl)guanine-9-acetyl-[(9² → 8²-N)-8-(2-aminoethyl)guanine-9-acetyl]₃-(9² → 6²-N)-6-(2-aminoethyl)cytosine-1-acetyl-[(1² → 6²-N)-6-(2-aminoethyl)cytosine-1-acetyl]₃-I² → *Lys-Lys-NH*₂ (= N²-((6-[2-((6-[2-((6-[2-((8-[2-((8-[2-((8-[2-((8-[2-((8-[2-((8-[2-((Acetylamino)ethyl]-2-amino-6-oxo-1,6-dihydro-9H-purin-9-yl)acetyl)amino)ethyl]-2-amino-6-oxo-1,6-dihydro-9H-purin-9-yl)acetyl)amino)ethyl]-2-amino-6-oxo-1,6-dihydro-9H-purin-9-yl)acetyl)amino)ethyl]-4-((benzyloxy)carbonyl)amino)-2-oxopyrimidin-1(2H)-yl)acetyl)amino)ethyl]-4-((benzyloxy)carbonyl)amino)-2-oxopyrimidin-1(2H)-yl)acetyl)amino)ethyl]-4-((benzyloxy)carbonyl)amino)-2-oxopyrimidin-1(2H)-yl)acetyl)-L-lysyl-L-lysylamide; **54**). Similarly to the solid-phase synthesis of **30**, **54** was obtained by sequential double coupling (4 × **47** (35.5 mg, 62.5 μmol) and 4 × **49** (29.7 mg, 62.5 μmol) in the presence of HATU (22.8 mg, 60.0 μmol) and EtNⁱPr₂ (22 μl, 125 μmol) in DMSO (0.25 ml) for 8–10 h at 35° and 310 rpm on a *Rink* amide MBHA resin (34.7 mg, 25 μmol). The amino acid **44** (58.6 mg, 125 μmol) was sequentially doubly coupled (2 × 30 min with HATU (46.6 mg, 122.5 μmol) and EtNⁱPr₂ (44 μl, 250 μmol) in DMSO (0.25 ml)). The order of the couplings can be read from the sequence (C → N terminus). The crude product was cleaved from the support and not purified. Yellow powder. HPLC/MS (*Waters Atlantis dC18-3*, 100 × 3 mm; MeCN/H₂O/HCO₂H 10:90:0.1 → 95:5:0.1; flow: 0.2 ml/min; *Finnigan LCQ Deca Ion Trap* ESI-MS): *t*_R 19.5 min (1284 (100, [M + 2 H]²⁺)).

N-Acetyl-Lys-Lys-(→ 8²-N)-8-(2-aminoethyl)guanine-9-acetyl-[(9² → 8²-N)-8-(2-aminoethyl)guanine-9-acetyl]₃-(9² → 6²-N)-6-(2-aminoethyl)cytosine-1-acetyl-[(1² → 6²-N)-6-(2-aminoethyl)cytosine-1-acetyl]₃-I² → *Lys-Lys-NH*₂ (= N²-((6-[2-((6-[2-((6-[2-((8-[2-((8-[2-((8-[2-((8-[2-((8-[2-((Acetyl-L-lysyl-L-lysylamino)ethyl]-2-amino-6-oxo-1,6-dihydro-9H-purin-9-yl)acetyl)amino)ethyl]-2-amino-6-oxo-1,6-dihydro-9H-purin-9-yl)acetyl)amino)ethyl]-2-amino-6-oxo-1,6-dihydro-9H-purin-9-yl)acetyl)amino)ethyl]-4-((benzyloxy)carbonyl)amino)-2-oxopyrimidin-1(2H)-yl)acetyl)amino)ethyl]-4-((benzyloxy)carbonyl)amino)-2-oxopyrimidin-1(2H)-yl)acetyl)amino)ethyl]-4-((benzyloxy)carbonyl)amino)-2-oxopyrimidin-1(2H)-yl)acetyl)-L-lysyl-L-lysylamide; **55**). Similarly to the solid-phase synthesis of **30**, **55** was obtained by sequential double coupling (4 × **47** (35.5 mg, 62.5 μmol) and 4 × **49** (29.7 mg, 62.5 μmol)) in the presence of HATU (22.8 mg, 60.0 μmol) and EtNⁱPr₂ (22 μl, 125 μmol) in DMSO (0.25 ml) for 8–10 h at 35° and 310 rpm on a *Rink* amide MBHA resin (34.7 mg, 25 μmol). The amino acid **44** (58.6 mg, 125 μmol) was sequentially double coupled (4 × 30 min with HATU (46.6 mg, 122.5 μmol) and EtNⁱPr₂ (44 μl, 250 μmol) in DMSO (0.25 ml)). The order of the couplings can be read from the sequence (C → N terminus). The crude product was cleaved from the support and not purified. Yellow powder. HPLC/MS (*Waters Atlantis dC18-3*, 100 × 3 mm; MeCN/H₂O/HCO₂H 10:90:0.1 → 95:5:0.1; flow: 0.2 ml/min; *Finnigan LCQ Deca Ion Trap* ESI-MS): *t*_R 17.9 min (942 (100, [M + 3 H]³⁺)).

N-Acetyl-Asp-Asp-(→ 8²-N)-8-(2-aminoethyl)guanine-9-acetyl-[(9² → 8²-N)-8-(2-aminoethyl)guanine-9-acetyl]₃-(9² → 6²-N)-6-(2-aminoethyl)cytosine-1-acetyl-[(1² → 6²-N)-6-(2-aminoethyl)cytosine-1-acetyl]₃-I² → *Lys-Lys-NH*₂ (= N²-((6-[2-((6-[2-((6-[2-((8-[2-((8-[2-((8-[2-((8-[2-((8-[2-((Acetyl-L-aspartyl-L-aspartylamino)ethyl]-2-amino-6-oxo-1,6-dihydro-9H-purin-9-yl)acetyl)amino)ethyl]-2-amino-6-oxo-1,6-dihydro-9H-purin-9-yl)acetyl)amino)ethyl]-2-amino-6-oxo-1,6-dihydro-9H-purin-9-yl)acetyl)amino)ethyl]-4-((benzyloxy)carbonyl)amino)-2-oxopyrimidin-1(2H)-yl)acetyl)amino)ethyl]-4-((benzyloxy)carbonyl)amino)-2-oxopyrimidin-1(2H)-yl)acetyl)amino)ethyl]-4-((benzyloxy)carbonyl)amino)-2-oxopyrimidin-1(2H)-yl)acetyl)-L-lysyl-L-lysylamide; **56**). Similarly to the solid-phase synthesis of **30**, **56** was obtained by sequential double coupling (4 × **47** (35.5 mg, 62.5 μmol) and 4 × **49** (29.7 mg, 62.5 μmol)) in the presence of HATU (22.8 mg, 60.0 μmol) and EtNⁱPr₂ (22 μl, 125 μmol) in DMSO (0.25 ml) for 8–10 h at 35° and 310 rpm on a *Rink* amide MBHA resin (34.7 mg, 25 μmol). The amino acids **44** (58.6 mg, 125 μmol) and **45** (51.4 mg, 125 μmol) were sequentially doubly coupled (2 × 30 min with HATU (46.6 mg, 122.5 μmol) and EtNⁱPr₂ (44 μl, 250 μmol)

in DMSO (0.25 ml)). The order of the couplings can be read from the sequence (C → N terminus). The crude product was cleaved from the support and not purified. Yellow powder. HPLC/MS (*Waters Atlantis dC18-3*, 100 × 3 mm; MeCN/H₂O/HCO₂H 10 : 90 : 0.1 → 95 : 5 : 0.1; flow: 0.2 ml/min; *Finnigan LCQ Deca Ion Trap* ESI-MS): *t*_R 19.5 min (933 (100, [M + 3 H]³⁺)).

REFERENCES

- [1] L. Herdeis, B. Bernet, A. Augustine, R. E. Kälin, A. W. Brändli, A. Vasella, *Helv. Chim. Acta* **2011**, *94*, 545.
- [2] M. Peifer, F. De Giacomo, M. Schandl, A. Vasella, *Helv. Chim. Acta* **2009**, *92*, 1134.
- [3] X. M. Zhang, B. Bernet, A. Vasella, *Helv. Chim. Acta* **2007**, *90*, 864.
- [4] A. Ritter, D. Egli, B. Bernet, A. Vasella, *Helv. Chim. Acta* **2008**, *91*, 673.
- [5] K. Chiesa, A. Shvoryna, B. Bernet, A. Vasella, *Helv. Chim. Acta* **2010**, *93*, 668.
- [6] W. Czechtizky, A. Vasella, *Helv. Chim. Acta* **2001**, *84*, 1000.
- [7] Z. M. Zhang, B. Bernet, A. Vasella, *Helv. Chim. Acta* **2007**, *90*, 891.
- [8] X. M. Zhang, B. Bernet, A. Vasella, *Helv. Chim. Acta* **2006**, *89*, 2861.
- [9] A. J. Matthews, P. K. Bhardwaj, A. Vasella, *Helv. Chim. Acta* **2004**, *87*, 2273.
- [10] W. Czechtizky, A. Vasella, *Helv. Chim. Acta* **2001**, *84*, 594.
- [11] H. Gunji, A. Vasella, *Helv. Chim. Acta* **2000**, *83*, 2975.
- [12] S. Eppacher, N. Solladie, B. Bernet, A. Vasella, *Helv. Chim. Acta* **2000**, *83*, 1311.
- [13] R. B. Merrifield, *J. Am. Chem. Soc.* **1963**, *85*, 2149.
- [14] R. L. Letsinger, V. Mahadevan, *J. Am. Chem. Soc.* **1965**, *87*, 3526; M. Beier, F. Reck, T. Wagner, R. Krishnamurthy, A. Eschenmoser, *Science* **1999**, *283*, 699; K. U. Schöning, P. Scholz, S. Guntha, X. Wu, R. Krishnamurthy, A. Eschenmoser, *Science* **2000**, *290*, 1347.
- [15] M. Egholm, O. Buchardt, P. E. Nielsen, R. H. Berg, *J. Am. Chem. Soc.* **1992**, *114*, 1895; M. Egholm, P. E. Nielsen, O. Buchardt, R. H. Berg, *J. Am. Chem. Soc.* **1992**, *114*, 9677; M. Egholm, C. Behrens, L. Christensen, R. H. Berg, P. E. Nielsen, O. Buchardt, *J. Chem. Soc., Chem. Commun.* **1993**, 800; K. L. Dueholm, M. Egholm, C. Behrens, L. Christensen, H. F. Hansen, T. Vulpius, K. H. Petersen, R. H. Berg, P. E. Nielsen, O. Buchardt, *J. Org. Chem.* **1994**, *59*, 5767; P. Wittung, M. Eriksson, R. Lyng, P. E. Nielsen, B. Norden, *J. Am. Chem. Soc.* **1995**, *117*, 10167.
- [16] S. A. Thomson, J. A. Josey, R. Cadilla, M. D. Gaul, C. F. Hassman, M. J. Luzzio, A. J. Pipe, K. L. Reed, D. J. Ricca, R. W. Wiethe, S. A. Noble, *Tetrahedron* **1995**, *51*, 6179.
- [17] P. K. Bhardwaj, A. Vasella, *Helv. Chim. Acta* **2002**, *85*, 699.
- [18] L. A. Marky, K. J. Breslauer, *Biopolymers* **1987**, *26*, 1601; R. Owczarzy, *Biophys. Chem.* **2005**, *117*, 207; J. L. Mergny, L. Lacroix, *Oligonucleotides* **2003**, *13*, 515.
- [19] P. Yakovchuk, E. Protozanova, M. D. Frank-Kamenetskii, *Nucleic Acids Res.* **2006**, *34*, 564; K. M. Guckian, B. A. Schweitzer, R. X. F. Ren, C. J. Sheils, P. L. Paris, D. C. Tahmassebi, E. T. Kool, *J. Am. Chem. Soc.* **1996**, *118*, 8182; E. T. Kool, J. C. Morales, K. M. Guckian, *Angew. Chem., Int. Ed.* **2000**, *39*, 990.
- [20] P. E. Nielsen, M. Egholm, R. H. Berg, O. Buchardt, *Science* **1991**, *254*, 1497.
- [21] G. R. Desiraju, *Angew. Chem., Int. Ed.* **2011**, *50*, 52; G. R. Desiraju, *Acc. Chem. Res.* **1991**, *24*, 290.
- [22] H. Rink, *Tetrahedron Lett.* **1987**, *28*, 3787.
- [23] R. Knorr, A. Trezciak, W. Bannwarth, D. Gillessen, *Tetrahedron Lett.* **1989**, *30*, 1927.
- [24] L. A. Carpino, *J. Am. Chem. Soc.* **1993**, *115*, 4397; F. Albericio, J. M. Bofill, A. El-Faham, S. A. Kates, *J. Org. Chem.* **1998**, *63*, 9678.
- [25] O. Marder, Y. Shvo, F. Albericio, *Chim. Oggi – Chem. Today* **2002**, *20*, 37.
- [26] J. Martinez, J. P. Bali, M. Rodriguez, B. Castro, R. Magous, J. Laur, M. F. Lignon, *J. Med. Chem.* **1985**, *28*, 1874.
- [27] G. B. Fields, C. G. Fields, *J. Am. Chem. Soc.* **1991**, *113*, 4202.
- [28] A. Thaler, D. Seebach, F. Cardinaux, *Helv. Chim. Acta* **1991**, *74*, 617; A. Thaler, D. Seebach, F. Cardinaux, *Helv. Chim. Acta* **1991**, *74*, 628.
- [29] C. Hyde, T. Johnson, R. C. Sheppard, *J. Chem. Soc., Chem. Commun.* **1992**, 1573.

- [30] P. Sieber, *Tetrahedron Lett.* **1987**, 28, 2107; W. C. Chan, S. L. Mellor, *J. Chem. Soc., Chem. Commun.* **1995**, 1475; W. C. Chan, P. D. White, J. Beythien, R. Steinhauer, *J. Chem. Soc., Chem. Commun.* **1995**, 589.
- [31] K. L. Dueholm, K. H. Petersen, D. K. Jensen, M. Egholm, P. E. Nielsen, O. Buchardt, *Bioorg. Med. Chem. Lett.* **1994**, 4, 1077.
- [32] T. Okawara, Y. Kanazawa, T. Yamasaki, M. Furukawa, *Synthesis* **1987**, 183.
- [33] W. Walter, K. J. Reubke, *Chem. Ber./Recl.* **1970**, 103, 2197; M. J. S. Dewar, W. B. Jennings, *J. Am. Chem. Soc.* **1973**, 95, 1562.
- [34] M. Egholm, O. Buchardt, P. E. Nielsen, R. H. Berg, *J. Am. Chem. Soc.* **1992**, 114, 1895.

Received March 23, 2011